THE UNIVERSITY OF DANANG
UNIVERSITY OF SCIENCE AND TECHNOLOGY
FACULTY OF TRANSPORT MECHANICAL ENGINEERING

GRADUATION PROJECT
CAPSTONE PROJECT

MECHANICAL ENGINEERING
MAJOR IN AUTOMOTIVE ENGINEERING

RESEARCH TOPIC:

A STUDY ON THE KINEMATICS OF 3-D DOUBLE-CONCENTRIC JETS USING ANSYS FLUENT

****

(NGHIÊN CỨU ĐỘNG HỌC TIA PHUN KÉP 3D KẾT HỢP XUNG NHỊP BẰNG PHƯƠNG PHÁP MÔ PHỎNG SỐ SỬ DỤNG ANSYS FLUENT)

Supervisor: **Assoc. Prof. Dr. Le Minh Duc**
Student: **Huynh Tan Huy**
Student ID**: 103200156**
Class: **20C4CLC3**

Da Nang, 06/2025

NHẬN XÉT CỦA NGƯỜI HƯỚNG DẪN

ABSTRACT

Research title: A study on kinematics of 3-D double-concentric jets using Ansys Fluent

Student researcher: Huynh Tan Huy

Student ID number: 10320156 Class: 20C4CLC3

The research topic focuses on evaluating the influence of parameters such as the velocity ratio between the fuel stream and the air stream on flow structure, vortex formation, and mixing capability in a dual-jet nozzle. The study is built upon various specialized technical knowledge to support calculations and simulations.

Chapter 1: Overview. This section presents the theoretical background, research objectives, research subjects, as well as the research methodology and scope of the study.

Chapter 2: Methodologies. This chapter presents the overall research procedure, detailing the working principle of the jet nozzle and the calculation of parameters for each simulation case. It introduces the ANSYS Fluent software and describes the simulation workflow, including an analysis of the turbulence models used.

Chapter 3: Analysis of simulation results by constructing graphs based on simulated cases, and comparing continuous and pulsed injection modes to draw conclusions on mixing efficiency**.**

Chapter 4: Conclusion and Future Study

PREFACE

In recent years, energy-saving and improving combustion system efficiency in engines and industrial combustion chambers have gained increasing attention. In particular, the enhancement and optimization of fuel injection systems to improve mixing performance, increase combustion efficiency, and reduce emissions have become a central focus in various engineering fields.

One of the promising solutions under research is the use of double jet nozzle structures, which generate strong vortices and optimize the distribution of fuel and air within the combustion chamber. Evaluating the effects of the velocity ratio between fuel and air streams, as well as the geometry of the bluff body, on flow fields, vortex formation, and mixing processes is a key factor in designing an efficient injection system.

From this practical demand, I decided to carry out the research topic:**“** A study on kinematics of 3-D double-concentric jets using Ansys Fluent**”**

Through the implementation of this project, I not only reinforced my knowledge in fluid dynamics and turbulence modeling but also improved my skills in numerical simulation, data processing, and analytical thinking. This serves as a solid foundation for my personal development and prepares me to apply this knowledge effectively in real-world engineering work in the future.

However, due to limited time and my own knowledge constraints, shortcomings in the process of conducting this study are inevitable. I would like to sincerely thank Associate Professor Dr.Le Minh Duc for his dedicated guidance throughout the implementation of this project. I respectfully look forward to receiving feedback from the lecturers to further improve this research.

DECLARATION

I hereby declare that the thesis titled **"**Research on 3d double jet dynamics combining pulsating using numerical simulation method with ansys fluent**"** was carried out with the guidance and support of my academic supervisor, as well as knowledge gathered from reference materials. Therefore, this thesis upholds academic integrity.

Student

Huynh Tan Huy

TABLE OF CONTENTS

LIST OF TABLES AND FIGURES

LIST OF SYMBOLS AND ABBREVIATIONS

ABBREVIATIONS:

RANS: Reynolds-Averaged Navier–Stokes

CFD : Computational Fluid Dynamics

LES : Large Eddy Simulation

Re : Reynolds number

SGS : Subgrid-Scale

INTRODUCTION

In the context of increasing demands for fuel efficiency and emission control, the study and optimization of combustion processes in engine and combustion chamber systems have become critically important. One of the key factors influencing combustion performance is the spray and mixing characteristics of fuel with air. In this regard, the dual-jet nozzle is considered an effective engineering solution to enhance fuel-air mixing, improve combustion efficiency, and reduce harmful emissions.

Numerical simulation plays a vital role in analyzing and understanding the complex dynamic processes occurring within the spray region. With its capability to handle turbulent, time-dependent, and spatially varying flow problems, ANSYS Fluent enables detailed investigation of 3D spray behavior under various conditions, such as continuous and pulsed injection. This allows for the observation of key characteristics, including vortex structures, jet development, and velocity distribution.

The research focuses on modeling a three-dimensional dual-jet nozzle with time-dependent pulsed velocity boundary conditions. The Reynolds-Averaged Navier–Stokes (RANS) approach is employed to capture large-scale vortex structures, combined with the Species Transport model to analyze gas mixing behavior. The simulation results provide both quantitative and visual insights into the spray process, serving as a foundation for evaluating the performance and optimizing the operation of the dual-jet nozzle system.

CHAPTER 1: OVERVIEW

1.1. Theoretical background

1.1.1. Fluid mechanics engineering

In the Fluid mechanics course, students are equipped with fundamental knowledge about the flow of liquids and gases in engineering systems, particularly those involving the transport of mass, energy, and momentum. This is one of the core foundational subjects in the field of Automotive and Mechanical Engineering, providing deeper insights into flow phenomena in pipelines, nozzles, turbines, pumps, and especially processes related to jet flow, pulsation, and mixing [2].

Based on this knowledge, one can directly apply it to the analysis and simulation of jet flows under complex engineering conditions—such as analyzing jet characteristics including propagation velocity, core region, mixing region, and flow instability. Through the Reynolds number, it is possible to identify whether a flow is laminar or turbulent. Additionally, it allows for the analysis of momentum exchange between fluid or gas streams when they intersect or interact with one another [2].

1.1.2. Advanced fluid dynamics

The Advanced fluid dynamics course provides both foundational and in-depth knowledge of fluid mechanics under more complex conditions compared to basic fluid mechanics. This course plays a vital role in understanding and analyzing real-world phenomena such as turbulent flow, nonlinear motion, compressible and incompressible flows, and mass–heat exchange processes in environments with significant variations in kinetic energy and pressure [3].

Turbulent flow analysis is essential, as turbulence commonly occurs in jet flows and fuel–air mixing processes. Understanding the structure of turbulence, statistical characteristics, and modeling approaches such as RANS (Reynolds-Averaged Navier–Stokes) and LES (Large Eddy Simulation) allows accurate simulation of mass and momentum transport in the jet region [3].

The Navier–Stokes equations are the fundamental set of equations that describe the motion of fluids and gases, serving as the core of all flow simulation problems. In CFD (Computational Fluid Dynamics) simulations, this system of equations is solved to determine the distribution of velocity, pressure, and related parameters throughout the computational domain [3].

Turbulence phenomena and the interaction between jet streams help explain the formation of strong mixing zones between air and fuel jets.

A key dimensionless parameter—the Reynolds number (Re)—characterizes whether a flow is laminar or turbulent. In the study, Re is used to determine injection conditions, turbulence scale, and to select appropriate computational models [3].

1.1.3. Theory of spray phenomena and mixing process

The injection process occurs when fuel is sprayed at high pressure through small nozzle orifices, forming fine jets or mist-like droplets. The jet flow is typically turbulent and is governed by parameters such as jet velocity, nozzle geometry, pressure differential, and the surrounding environment. Variations in pulse frequency or jet speed influence the development of the mixing region, mixing efficiency, and combustion duration [4].

Mixing is the process of diffusion and convection between fuel and air, which depends on flow turbulence, inertia, and viscosity mechanisms. In 3D CFD simulations, investigating turbulence and flow structure development at the intersection region of fuel jets plays a key role in accurately predicting combustion performance and efficiency, thereby offering insights into how injector performance can be improved [4].

In the Internal Combustion Engine course, the injection and mixing processes between fuel and air are considered crucial factors affecting combustion efficiency and pollutant emissions. The mixing process is influenced by several factors such as spray angle, injection pressure, and nozzle geometry. Mixing efficiency is evaluated through the uniformity of the air–fuel mixture, also referred to as the local equivalence ratio. Jet velocity influences the penetration capability and turbulence level of the fuel stream. Based on this knowledge, the effectiveness of mixing and the combustion potential can be assessed in the current simulation study [1].

1.1.4. 3D-CFD modeling in the calculation and simulation of the mixing process in a jet nozzle

Today, 3D-CFD (Computational Fluid Dynamics) theory has become a powerful and practical tool for solving problems related to the dynamics and physico-chemical properties of fluid flows in complex environments one of which is the simulation of jet mixing processes. In simulations involving the mixing of fuel and air jets, combustion and flow mixing are calculated based on flame propagation in the medium and local heat release, which depends on the combustion intensity in each region [5].

In the turbulent flame model, the flame structure is characterized by vortex formations. In a dual-jet injector model, the interaction between two air and fuel streams, combined with the effect of a secondary bluff-body disk, generates strong vortices, significantly enhancing the mixing interface and thereby increasing diffusion efficiency and mixing rate [5].

3D simulation represents the most advanced numerical approach for detailed investigation of thermodynamic problems in fluid mechanics. This method relies on numerical solutions of partial differential equations governing mass, species concentration, momentum, and energy conservation over an arbitrary fluid domain (Eulerian formulation). While the fundamental conservation equations have been known since the 19th century, their numerical implementation in computer-based simulations of fluid dynamics problems has only become feasible in recent decades [5].

With the emergence of high-speed computing since the late 1980s, numerical solutions of complex fluid domains have become achievable. To enable computers to solve fluid or gas domains continuously, these domains must be represented as a finite number of discrete elements often numbering in the millions. The most common discretization technique is to divide the domain into smaller subregions or elements (finite volume approximation), forming a mesh of elements known as a computational grid. This mesh provides the framework for localized numerical solutions of the discretized governing equations, which are solved using differential equation systems in simulation [5].

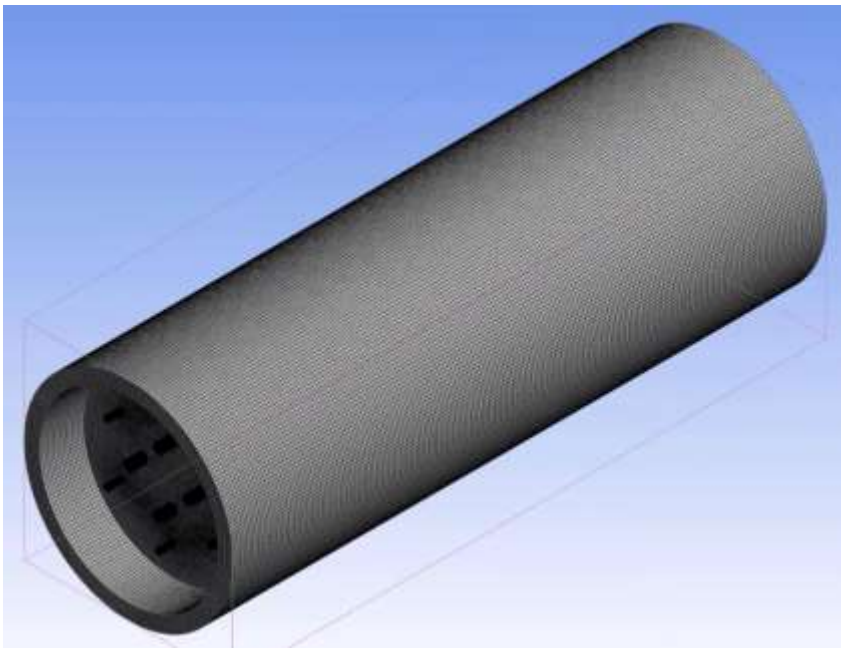

Figure 1.1 3D-CFD Mesh Model of the Combustion Chamber

This mesh serves as a framework for the localized numerical solution of the discretized governing equations, which are solved using systems of differential equations applied in simulations.

Some differential equations used in 3D-CFD simulations include:

The conservation equations of fluid dynamics, which serve as the starting point for simulation and represent the fundamental equations for any thermodynamic system. The conservation equation of an extensive variable $F(t)$ can be expressed in the following general form (Eulerian formulation) [6]:

$$\frac{\partial f}{\partial t} + div \cdot \vec{\Phi}_f = s_f + c_f \qquad (1.1)$$

Where: $f(\vec{x},t) = \frac{dF}{dV}$ is the density of the corresponding variable or the intensive variable of F(t) in the control volume element at position $\vec{x}$. The conservation equation shows that the change in the density of variable $f(\vec{x},t)$ may result from a flow $\vec{\Phi}_f \cdot \vec{n} dS$ through the surface of the control volume element, through a process of generation or depletion s_f and external source addition c_f.. From this general formulation, the conservation equations for mass, momentum, energy, and species can be established.

Species Mass Conservation Equation in the case of the mass fraction $w_i = \frac{m_i}{m}$ of species i, the variable density corresponds to the mass density ρi of species i. The local flow velocity $\vec{v}_i$ consists of the mean flow velocity $\vec{v}$ and the diffusion velocity $\vec{V}_i$. The diffusion flux generates a diffusive mass flow $\vec{j}_i$. Species can also be formed and destroyed in chemical reactions, such as combustion processes, when the fuel and air jets interact [6].

$$f = \rho_i = \rho w_i, \quad \vec{\Phi}_f = \rho_i \vec{V}_i = \rho_i \left(\vec{v} + \vec{v}_i\right) = \rho_i \vec{v} + \vec{j}_i, \quad s_f = M_i \omega_i, \quad c_f = 0 \qquad (1.2)$$

$$\frac{\partial(\rho w_i)}{\partial t} + \nabla \cdot (\rho w_i \vec{v}) + \nabla \cdot \vec{j}_j = M_i \omega_i \qquad (1.3)$$

Where: M_i and ω_i is the mol mass and the mol formation rate of species i resulting from the corresponding chemical reaction.

Mass Conservation Equation When calculating, the software considers the mass m f the control volume as the variable F(t), the rate of change $f(\vec{x},t)$ is given by the

mass density ρ và and the flux density is the product of the local flow velocity $\vec{v}$ and ρ [6]. Since mass cannot be created or destroyed within the flow, the following relationships apply:

$$f = \rho, \quad \vec{\Phi}_f = \rho\vec{v}, \quad s_f = 0, \quad c_f = 0 \tag{1.4}$$

$$\frac{\partial \rho}{\partial t} + \mathrm{div}(\rho\vec{v}) = 0 \tag{1.5}$$

The Navier-Stokes equations are the momentum equations in fluid mechanics, represented as a system of partial differential equations for liquids and gases, collectively referred to as fluids. These equations describe the balance of momentum and the conservation of mass in a fluid. They have widespread applications and are commonly used to simulate weather patterns, ocean currents, airflow in pipes, and various studies on fluid flow [6].

In the case of momentum conservation, the general form of density is replaced by momentum density $\rho\vec{v}$, Momentum flux includes a first-order component represented by convection: $\rho\vec{v} \otimes \vec{v}$ and a second-order term, which is the stress field $\bar{\bar{P}}$ (a tensor) describe the change in momentum due to viscosity $\bar{\bar{\Pi}}$ (surface tension) nd pressure, and may also account for the effect of gravity $\rho\vec{g}$, as follows:

$$f = \rho\vec{v}, \quad \vec{\Phi}_f = \rho\vec{v} \otimes \vec{v} + \bar{\bar{P}}, \quad s_f = 0, \quad c_f = \rho\vec{g} \tag{1.6}$$

Where: $\bar{\bar{P}} = p\bar{\bar{I}} + \bar{\bar{\Pi}}$

Therefore, the general formula is: $\frac{\partial(\rho\vec{v})}{\partial t} + \mathrm{div}(\rho\vec{v} \otimes \vec{v}) + \mathrm{div}\,\bar{\bar{\Pi}} - \nabla p = \rho\vec{g}$ (1.7)

1.2. Research objectives

Evaluation of the mixing efficiency between fuel and air under different injection modes, such as continuous injection, and the impact of the velocity ratio between the air and fuel jets on the mixing performance. In addition, the role of the bluff body (swirl-generating disk) in vortex formation is also investigated.

The optimal injection mode is identified by determining the velocity ratio between the two jets (fuel and air). Furthermore, a comparison is made between continuous and pulsed injection modes to assess which mode better optimizes mixing efficiency and enhances combustion performance.

1.3. Research subject

The dual injector is a type of device capable of simultaneously injecting both fuel and air, thereby optimizing the formation of the fuel–air mixture prior to combustion. The injector used in this study is a coaxial type. Additionally, it is equipped with a bluff body located at the front of the fuel nozzle.

Nowadays, dual injectors represent a modern technology that plays a crucial role in enhancing combustion efficiency, improving flame stability, and reducing fuel consumption. As a result, they are widely applied in various fields, including industrial and aerospace combustion chambers.

Dual injectors can be classified into several types based on configuration or injection media, with each type serving different functional purposes.

- Based on configuration:

  + Coaxial dual injectors feature a structure in which two nozzles are arranged concentrically—one flow passes through the central core while the other surrounds it and flows in the same direction. This design enables efficient mixing between the two streams, potentially enhancing combustion performance. This type of injector is commonly used in combustion chambers of jet engines and rockets.

  + Parallel dual injectors consist of two separate nozzles positioned side by side, injecting flows in nearly parallel directions. This configuration is often employed in experimental models to study the interaction between two fluid streams. As such, parallel injectors are typically used in scientific research and industrial combustion chambers.

- Based on the working fluids, dual injectors can be categorized into several types:

  + Gas–gas dual injectors: Both nozzles emit gas streams. This type iscommonl used for studying turbulent flows in aerodynamics.

  + Gas–liquid dual injectors: One nozzle emits gas while the other sprays liquid. This configuration is typically applied in combustion chambers and fuel injection.

Table 1.1 Typical Studies on Coaxial Jet Configurations

Order	Research Title	Author	Research Results	Research Methodology

1	Flow Characteristics and Velocity Fields of Swirling Double-concentric Jets at High Central Jet Reynolds Numbers	Minh Duc Le, Ching Min Hsu2, and Rong Fung Huang, 2018 [8]	Classification of two flow regimes: Jet-like regime: Dominated by the central jet at low Reynolds numbers, characterized by an expanding flow with a large shear layer due to the high velocity of the central jet. Swirl wake regime: Occurs at high Reynolds numbers of the annular jet, featuring the formation of a large double vortex wake downstream and two pairs of vortices between the control discs.	Experimental
2	Flow and Mixing Characteristics of Swirling Doubleconcentric Jets Modulated by a Dual-disk Controller	Rong Fung Huanga, Le Minh Duc, Ching Min Hsu 2015[9]	The study identified four characteristic flow regimes Wake region dominated by the annular jet appearing when the annular jet has a low Reynolds number. Wake region dominated by the central jet when the central jet has a high velocity. Jet-like flow dominated by the central jet, where a strong central jet creates a jet-like flow with an expanded shear layer. Swirl wake region with high turbulence intensity occurring when the annular jet has a high Reynolds number.	Experimental

3	Velocity fields and mixing properties of swirling double-concentric jets using two separated circular disks as center bodies	Le Minh Duc, Ching Min Hsu và Rong Fung Huang 2017 [10]	When using a single circular disk, the central jet passes through the recirculation zone without reversing direction, resulting in poor mixing between the central jet and the swirling annular jet. When two separate circular disks are used, the momentum of the central jet shifts from axial to radial direction, generating two characteristic flow regimes: a closed ring wake region and a reversed turbulent wake region. The mixing capability is significantly improved with the use of two disks, achieving a maximum enhancement of approximately 96% compared to using a single disk.	Experimental
4	Effects of swirling strength on flow characteristics of swirling double-concentric jets with a dual-disk flow controller	Rong Fung Huang, Le Minh Duc và Ching Min Hsu 2015 [11]	The results show that as the swirl intensity increases, the flow structure transitions from a jet-dominated wake region to a strongly turbulent swirling wake region. This swirling wake region exhibits significantly higher axial velocityand turbulence intensity, enhancing the mixing efficiency of the jet system.	Experimental
5	Swirling dual-disk double-concentric jets at	Le Minh Duc, Rong	The wake region dominated by the annular jet is mainly influenced by the annular jet,	Experimental

	low annulus Reynolds numbers.	Fung Huang, Duc và Ching Min Hsu 2017 [12]	featuring a stable wake with minimal swirling. The wake region dominated by the central jet exhibits a double recirculation zone at the rear and two pairs of counter-rotating vortices between the two discs, enhancing mixing between the central and annular jets. The radial flow driven by the central jet expands in the radial direction due to the high velocity of the central jet.	

From the above studies, it can be seen that most analyses of the mixing process of fluid flows, the effects of vortices, and the flow structure in dual concentric jet models with dual-disk control have been conducted through experimental methods. However, with the current support of CFD numerical simulations, the study of complex fluid phenomena has become more feasible and cost-effective. Therefore, in this research, a CFD simulation model is implemented to verify whether the obtained results are consistent with the trends observed in experiments, while also clarifying the role of simulations in gaining deeper insights into the mixing mechanisms and vortex structures in the dual-jet system.

1.4. Research methodology

RANS simulation of the combustion and kinetic mixing process between two fuel and air jets on a dual-nozzle model with a baffle plate, using Methane (CH4) as fuel and Oxygen (O2) as air. Simulations were carried out under varying injection velocities of fuel and air.

In combination, LES simulations of the non-combusting continuous injection mode were performed and compared with the pulsed injection mode results from previous studies. Both LES and RANS simulations were conducted using ANSYS Fluent 19.2 software.

1.5. Research scope.

The research focuses on studying the dynamics of a dual-jet spray in three-dimensional space, using ANSYS Fluent 19.2 to simulate and evaluate the mixing efficiency under continuous injection modes combined with varying velocity conditions. By comparing concentration distribution fields and the formation of turbulent vortex regions, the study aims to identify which injection mode or velocity ratio between fuel and air optimizes mixing efficiency, enhances combustion performance, and reduces harmful emissions.

CHAPTER 2: METHODOLOGIES

2.1. Structure and operating principle of the double jet nozzle

2.1.2. Operating pinciple of the coaxial double nozzle

During operation, the fuel flows through the central jet nozzle and is sprayed outward, while the air is injected from the outer nozzle. Because the dual nozzle is coaxial, the two streams of fuel and air are ejected in the same direction. Immediately after being sprayed, the air jet surrounds the fuel jet, which can have a significant impact on the diffusion of the fuel stream and increase the mixing time of the process.

At this point, thanks to the effect of the secondary baffle plate placed a certain distance in front of the fuel nozzle, a resistance zone is created. When the fuel is sprayed into this zone, it is forced to separate outward. Additionally, the primary plate also helps form vortex regions that enhance the mixing between air and fuel..

2.2. Simulation parameters

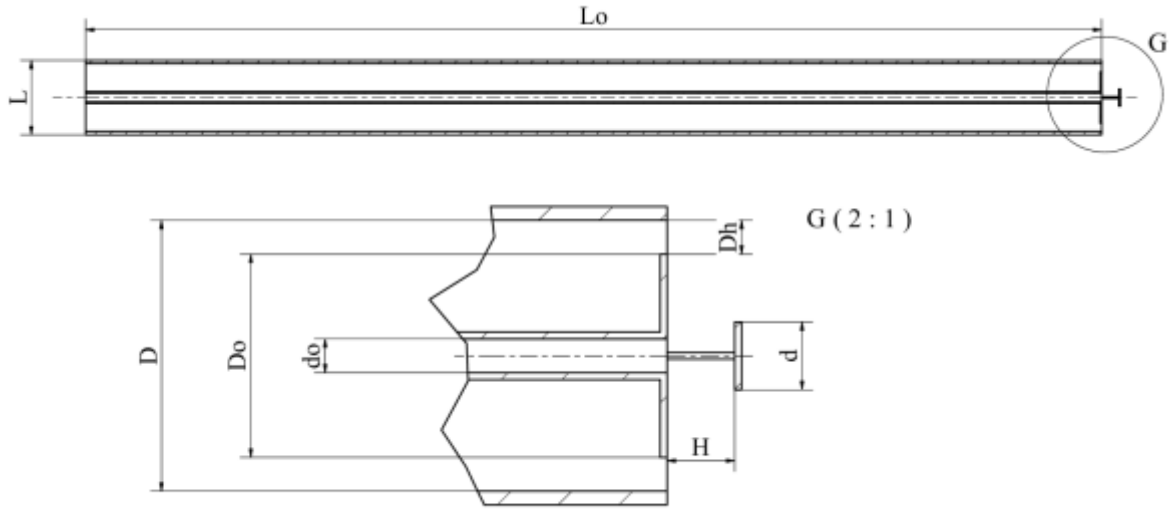

Figure 2.1 Description of the Dimensions of the Coaxial Double Nozzle

Based on the simulation problem parameters, the table below shows the dimensions of the dual nozzle used during the study:

Table 2.1 Dimensional Parameters of the Coaxial Double Nozzle

Name	Symbol	Value	Unit
Length of double jet nozzle body	L0	600	mm
Overall diameter of the double jet nozzle	L	44	mm
Outer diameter of the air jet	D	40	mm
Diameter of the primary disk	Do	30	mm
Diameter of the fuel jet	do	5	mm
Length of the support rod	H	10	mm
Diameter of the secondary disk	d= 2* do	10	mm
Exit diameter of the air nozzle	$D_H = D - D_o$	10	mm

2.1.1. Structure of the nozzle in the study

The dual nozzle used in this study is of the coaxial type with a simple structure, resembling two nested tubes. The inner tube is the central fuel injector, surrounded by an outer nozzle that sprays air. Notably, the nozzle in this study is equipped with two baffle plates: a primary plate and a secondary plate.

The primary plate is positioned immediately behind the air nozzle outlet. Its function is to reduce fluctuations and even out the spray flow, helping to prevent unwanted vortices or pulsations as the air flow exits the nozzle.

The secondary plate is placed a certain distance in front of the fuel nozzle. It plays a crucial role in creating a counteracting force region, which causes flow separation and generates vortices that enhance the mixing process between the air and fuel jets.

Support rods serve to hold and fix the secondary baffle plate in place, ensuring that it does not shift under the influence of high-pressure air flow.

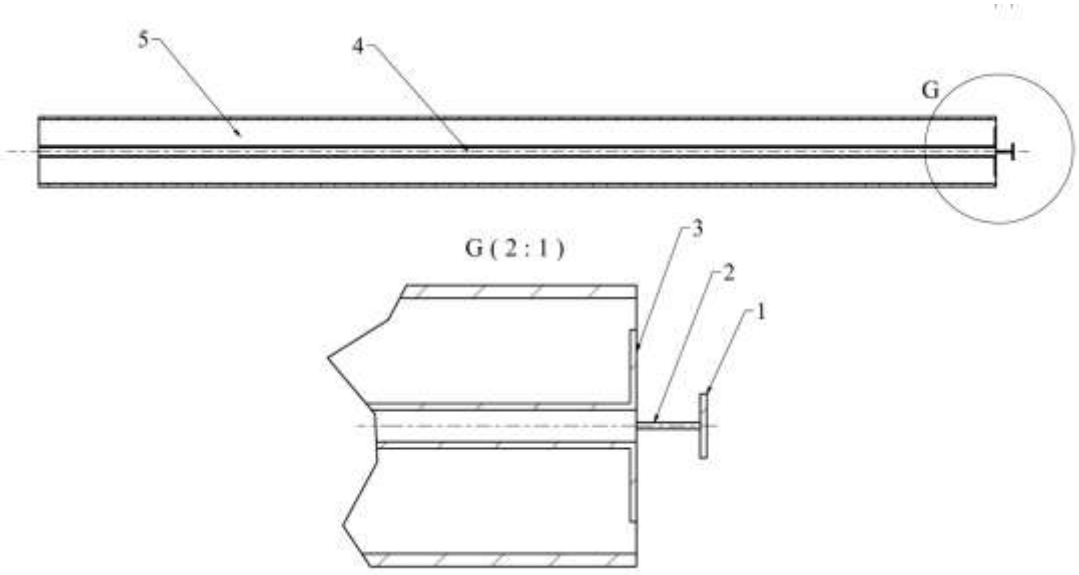

Figure 2.2 Structural Diagram of the Coaxial Dual-Jet Injector

1- Secondary disk; 2- Supporting rod; 3- Primary disk; 4- Central fuel injector; 5- Outer air injector

2.2.1. Calculation of parameters under continuous jet mode

Continuous jet mode means that the fuel and air flows are continuously supplied to the computational domain and maintained steadily over a long period of time. The velocity of the airflow exiting the nozzle is determined by the Reynolds number, with two specific cases considered Re_a= 1000 and Re_a= 5000.

The velocity of the airflow at the outlet of the coaxial nozzle is determined by applying the flow calculation formula for pipe flow:

$$Re_a = \frac{V_a D_H}{\nu} \quad (1.8)$$

Where :

Re_a : Reynolds number of the airflow

V_a : Velocity of airflow at the nozzle exit

ν : Kinematic viscosity of air assuming standard atmospheric conditions $\nu = 1.5*10^{-5}$ (m^2/s)

D_H : Diameter at the nozzle exit of the air jet

From this formula, the air velocity at the nozzle exit is calculated for different Reynolds number cases.

Case Re_a = 1000:

$$Re_a = \frac{V_a D_H}{\nu} \quad => \quad V_a = \frac{1000 * 1.5 * 10\text{^}(-5)}{0.01} = 1.5 \text{ (m/s)}$$

Case Re_a = 5000:

$$Re_a = \frac{V_a D_H}{\nu} \quad => \quad V_a = \frac{5000 * 1.5 * 10\text{^}(-5)}{0.01} = 7.5 \text{ (m/s)}$$

In addition to the two cases of air flow velocity, there are also three cases of fuel flow velocity, which is the premise for the simulation process to see how the effect between the velocity ratio of the two air and fuel flows will affect the mixing and combustion process of the dual nozzle. The table below shows the simulation cases corresponding to different values of the Reynold index:

Table 2.2 Simulation cases Re_a = 1000

Simulation case	Air jet velocity (V_a)	Fuel jet velocity (V_j)	Unit
Case 1	1.5	1	m/s
Case 2		2.5	m/s
Case 3		5	m/s

Table 2.3 Simulation cases Rea = 5000

Simulation case	Air jet velocity (V_a)	Fuel jet velocity (V_j)	Unit
Case 4	7.5	1	m/s
Case 5		2.5	m/s
Case 6		5	m/s

2.3. Build simulation process and 3D model of dual jet nozzle in ANSYS Fluent

2.3.1. Introduction to ANSYS Fluent 19.2

ANSYS Fluent 19.2 is a software with extensive modeling capabilities for fluid flow, turbulence, heat transfer and reaction models applied in industry and also widely used in research and design to optimize problems related to flow, heat transfer, chemical applications and many other complex physical phenomena. To do so, it is necessary to rely on special models in the software that have modeling capabilities, typically modeling cylinder engine combustion chambers, aerodynamics... and multiphase systems to serve to expand the software's capabilities.

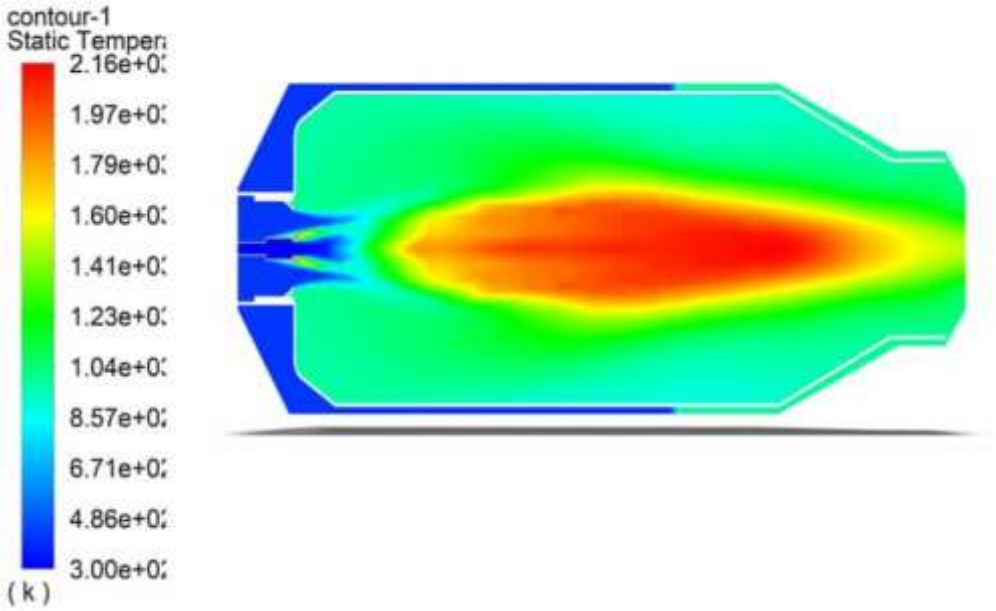

Figure 2.3 CFD simulation of combustion chamber using ANSYS Fluent

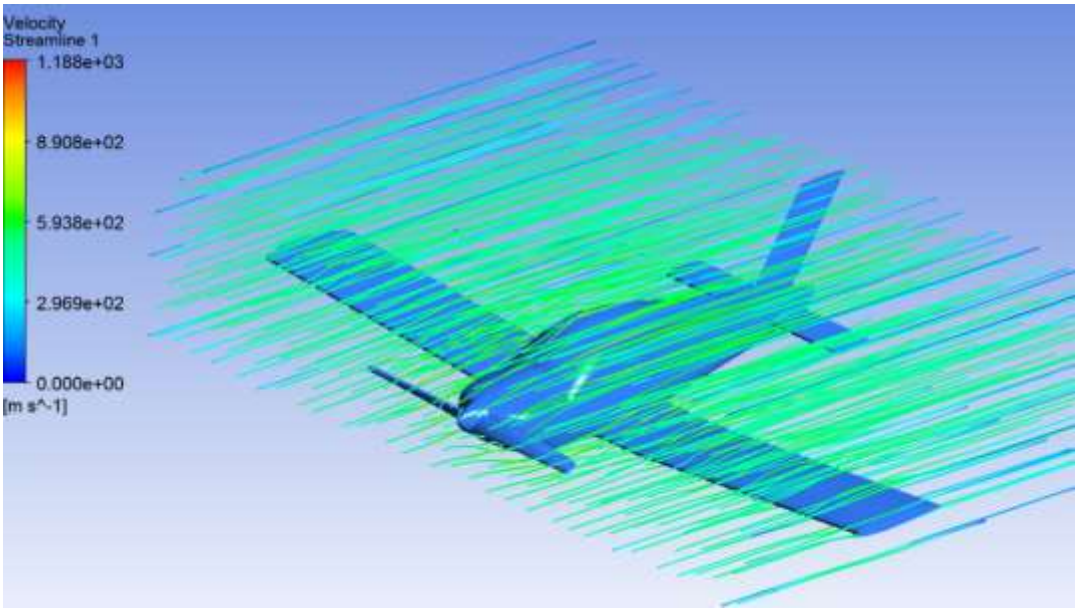

Figure 2.4 Aerodynamic simulation through aircraft using ANSYS Fluent

Today, ANSYS Fluent is an extremely important software for companies around the world, they use the software to simulate and analyze their products, thereby improving and optimizing the efficiency and product development process. Advanced engineering solvers help to provide fast and accurate results in different cases such as dynamic mesh or deformation and the ability to accelerate parallel running. The outstanding functions of this software are the modern user interface, allowing users to create and refine meshes directly in the Fluent environment without having to switch to a separate ANSYS Meshing, high computational performance to optimize the solving speed by algorithms significantly reducing simulation time, can combine models such

as chemical reaction models, turbulence models, radiation, heat transfer and phase transitions...

Combining a wide range of physical modeling capabilities and fast, accurate CFD results, ANSYS Fluent software delivers the most comprehensive software for CFD modeling available today.

2.3.2. Simulation process of dual jet nozzle in ANSYS Fluent

The simulation process of the dual nozzle is carried out in four stages:

- Geometric modeling of the dual nozzle is done using software such as Catia, SolidWorks, Inventor, or DesignModeler, which is a drawing module in ANSYS. After completing the model, it is converted into Step or IGES format to be imported into ANSYS for setting up the computational domain.
- Mesh generation can be done automatically or manually. After meshing, it is important to check the skewness, which is an index evaluating mesh quality. Poor quality or distorted mesh elements will be highlighted in red or yellow, allowing users to quickly identify and fix issues to ensure accuracy in the calculations
- Boundary condition setup is a crucial prerequisite to start the calculation and simulation process. This step involves setting velocity boundary conditions for the nozzles and selecting the appropriate computational model.
- Computation and post-processing involve running the simulation after setting boundary conditions and convergence parameters, including the number of iterations. After the simulation completes, the results such as velocity, pressure, and temperature fields are extracted for analysis.

2.3.3. Model construction

Based on the initial data from the geometric parameters of the dual nozzle, Inventor software is used to design the nozzle structure, which is then imported into ANSYS software. After importing, the computational domain—also called the calculation domain—is created. This domain represents the spatial region where the physical equations will be solved during the simulation to calculate variables such as velocity, temperature, and pressure.

In the nozzle simulation, the computational domain is the area where the fuel and air move, interact, and mix together. Additionally, this domain is where the mesh is generated and simulation results are displayed. Therefore, defining the flow domain is a critical step for the entire calculation process.

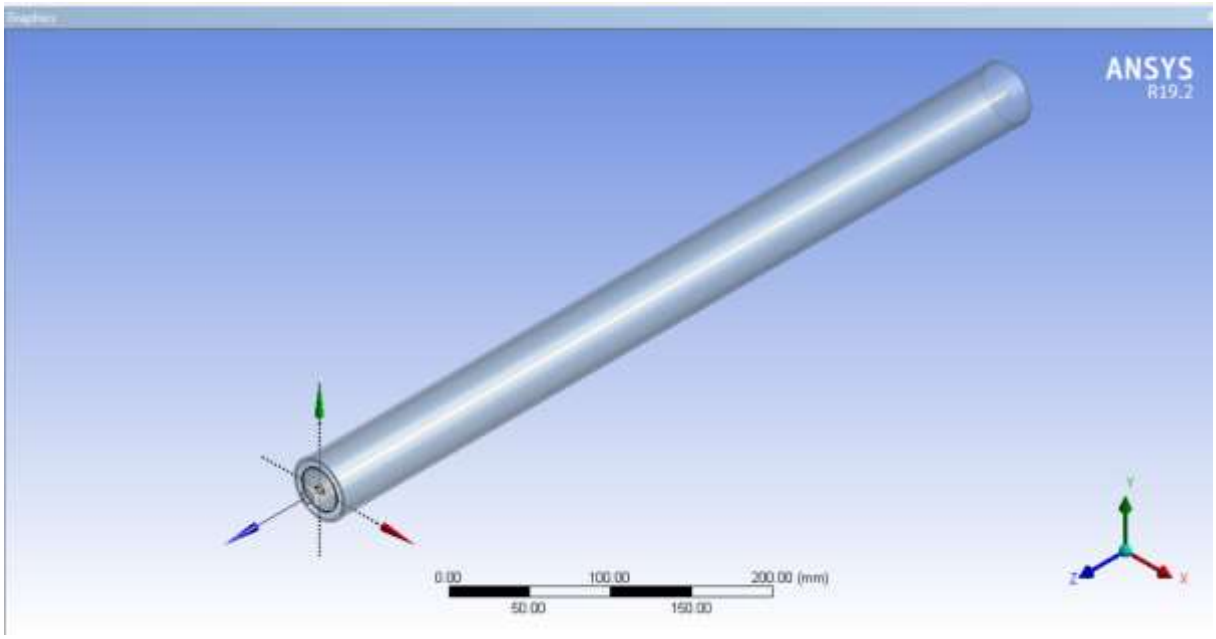

Figure 2.5 Dual jet nozzle imported into ANSYS Fluent

The computational domain in the simulation is a cubic region with dimensions of 400 x 400 x 400 mm. Depending on the type of object being simulated, the domain size should be adjusted accordingly. If the domain is chosen too small, the jet flow will not fully develop or form properly, leading to incomplete simulation of the mixing process between air and fuel, which causes inaccuracies in the results.

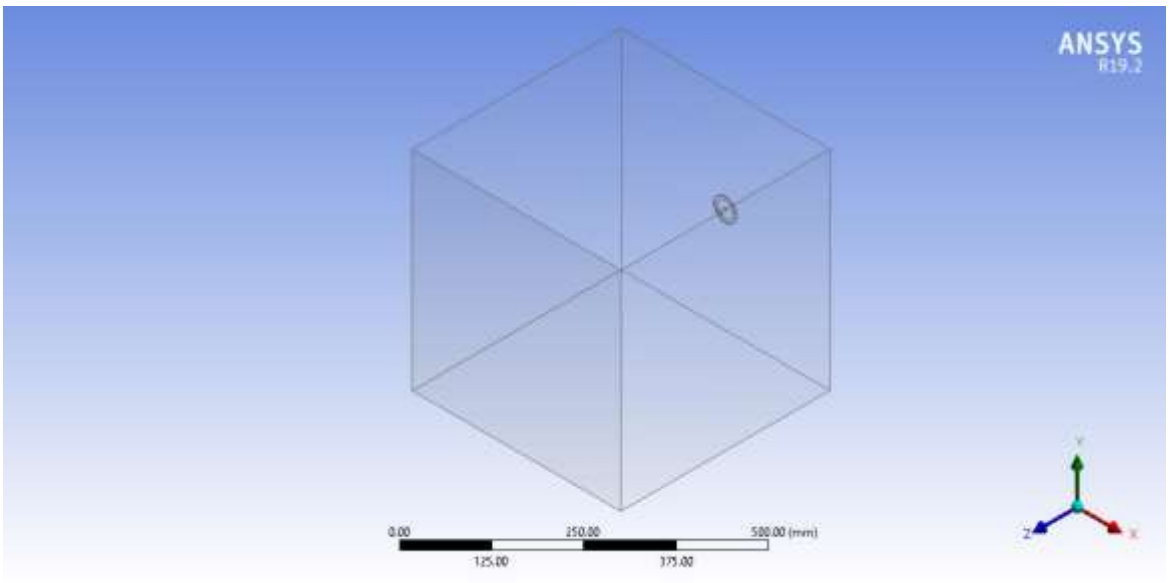

Figure 2.6 Domain model in ANSYS

Observing the computational domain model shows that only the portion from the nozzle tip, including the injection holes and the baffle discs, is retained while the nozzle body is omitted. The purpose of this is to reduce the number of mesh elements required

during the meshing step, thereby significantly decreasing computation time and saving computer resources.

Starting from the geometric model, the meshing process is performed using the Mesh tool. The meshing is done manually rather than automatically, allowing better control over mesh quality and customization of mesh types suitable for each model, which enhances the accuracy and stability of simulation results.

In the coaxial injector model, the most critical regions are the nozzle tip area and the zones near the secondary baffle disc, where strong vortices form. These areas require very fine mesh to accurately capture velocity variations during simulation, thus increasing the precision of the results. Regions farther away or with less variation in velocity or pressure can use coarser mesh to reduce the total number of elements and save computational resources. To achieve this, a combination of mesh refinement commands such as...

- Edge Sizing: This command divides the mesh along edges, assigning a specific number of elements based on the length of each edge. It ensures uniform and precise meshing in narrow regions such as the nozzle exit, where high resolution is necessary to accurately capture flow characteristics.
- Face Sizing: This command controls the mesh density on specific faces of the model, such as the surface of the baffle disk. It allows for finer mesh concentration in critical areas, improving simulation accuracy in zones with complex flow variations.
- Face Meshing: This command enforces structured mesh generation on faces, creating evenly distributed mesh elements based on parameters set by the Edge Sizing and Face Sizing commands. This ensures high-quality and uniform mesh on important surfaces, enhancing computational stability and accuracy.

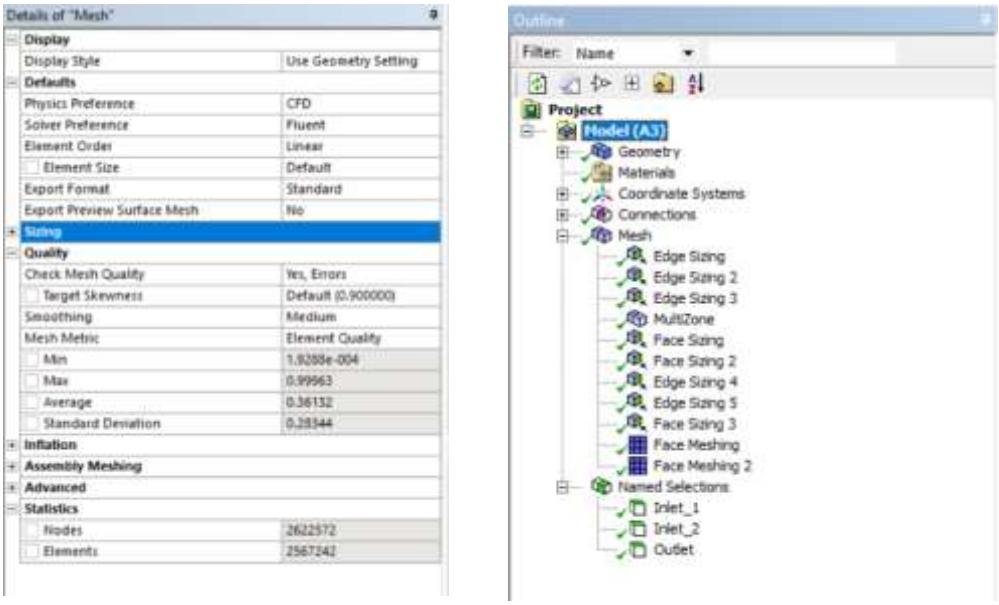

(a) (b)

Figure 2.7 Mesh parameters (a) and meshing commands (b) in Ansys

Table 2.4 Mesh size parameters

Order	Parameter		Value
1	Total number of nodes		2622572
2	Total number of elements		2567242
3	Element Quality	Min	$1.9288*10^{-4}$
		Max	0.99963
		Average	0.36132
4	Standard Deviation		0.28344
5	Minimum Edge Length (mm)		3.1416
6	Bounding Box Diagonal (mm)		693.4
7	Average Surface Area (mm^2)		50643

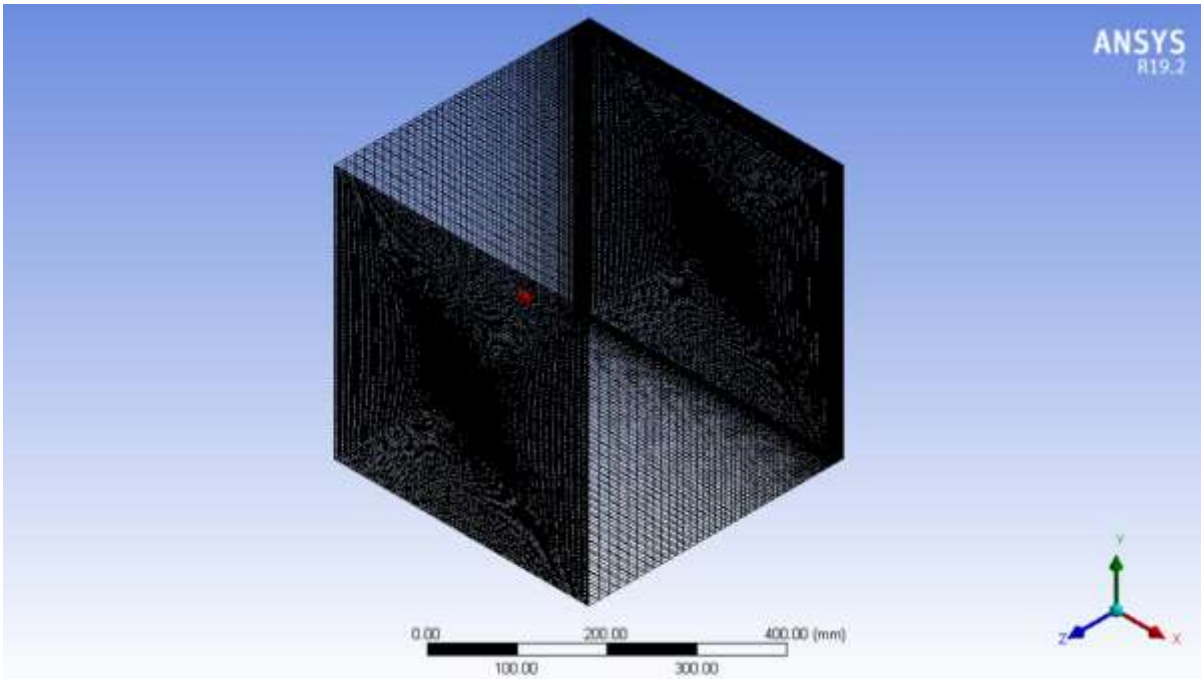

Figure 2.8 Meshing in Ansys

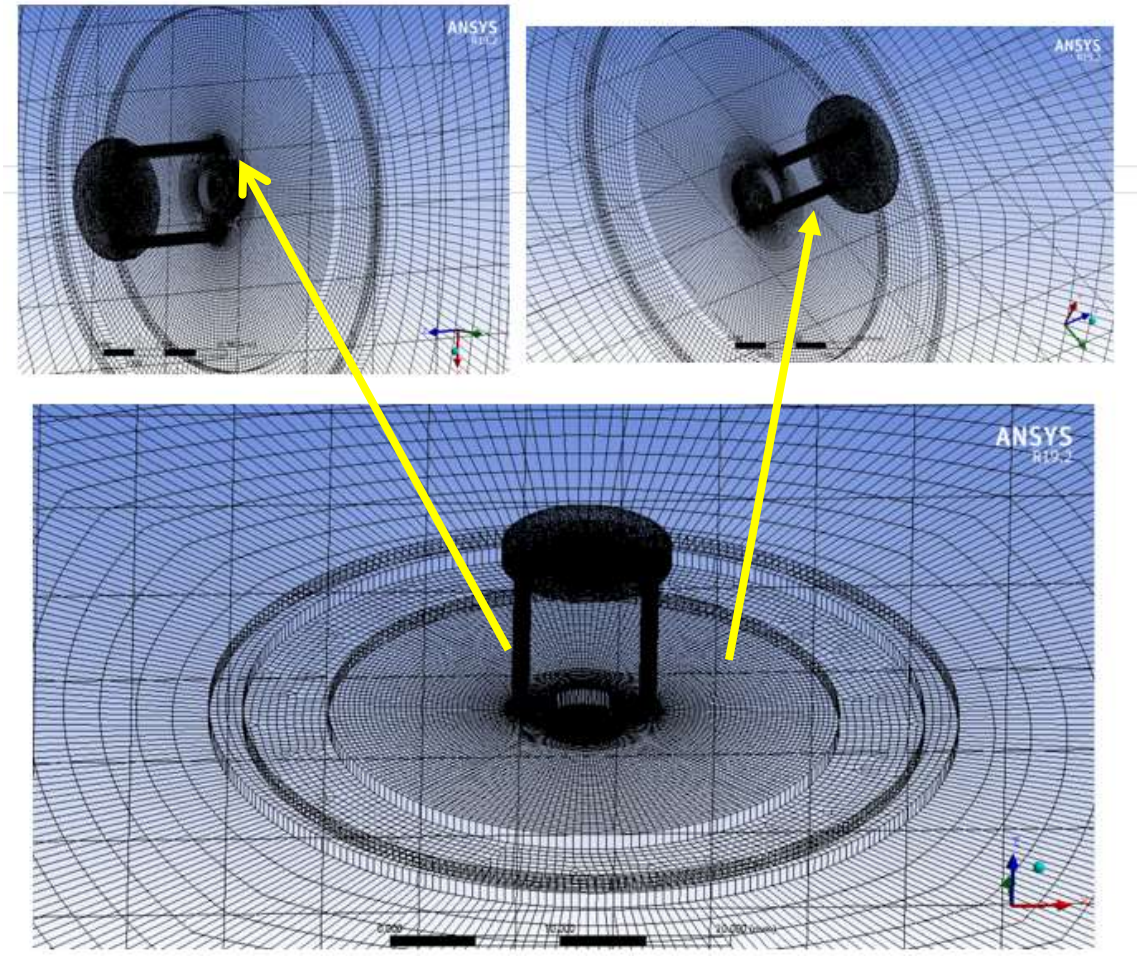

Figure 2.9 Meshing result of the nozzle

2.4. Simulation on Ansys Fluent

After completing the steps of building the Domain and dividing the mesh, proceed to set up the calculation model. In the simulation of dual nozzle CFD combined with combustion reaction, choosing the appropriate calculation model determines the accuracy of the problem. There are two basic types of models used in simulation studies: RANS (Reynolds-Averaged Navier–Stokes) model and LES (Large Eddy Simulation) model.

2.4.1. Setup in the RANS model

The RANS model, when solving problems, instead of directly simulating all turbulent structures in space and time, applies Reynolds averaging to the Navier–Stokes equations, thereby allowing direct solution of time-averaged quantities such as velocity, pressure, and temperature. This significantly reduces computational requirements, making it particularly suitable for engineering problems with large computational domains or high Reynolds number flows [7].

Therefore, the RANS model is chosen here to simulate the dual nozzle spray during mixing and combustion processes. This model solves the components of the mean velocity and models the effects through turbulence models such as k-epsilon and k-omega.

In the dual nozzle spray model, the Species Transport model is used to track the distribution of fuel and air concentrations as well as the products generated from the combustion process throughout the computational domain. Additionally, combustion models such as Premixed Combustion are used to simulate the assumption that fuel and air are completely mixed before combustion, with instantaneous reactions; Non-Premixed Combustion models allow fuel and air to meet in the mixing zone, with reactions controlled by diffusion. The Eddy Dissipation Model is selected to simulate the mixing in the dual nozzle spray when the two streams of air and fuel are injected, combining mass transport mechanisms and reaction rates, or assuming the reaction is limited by the mixing process.

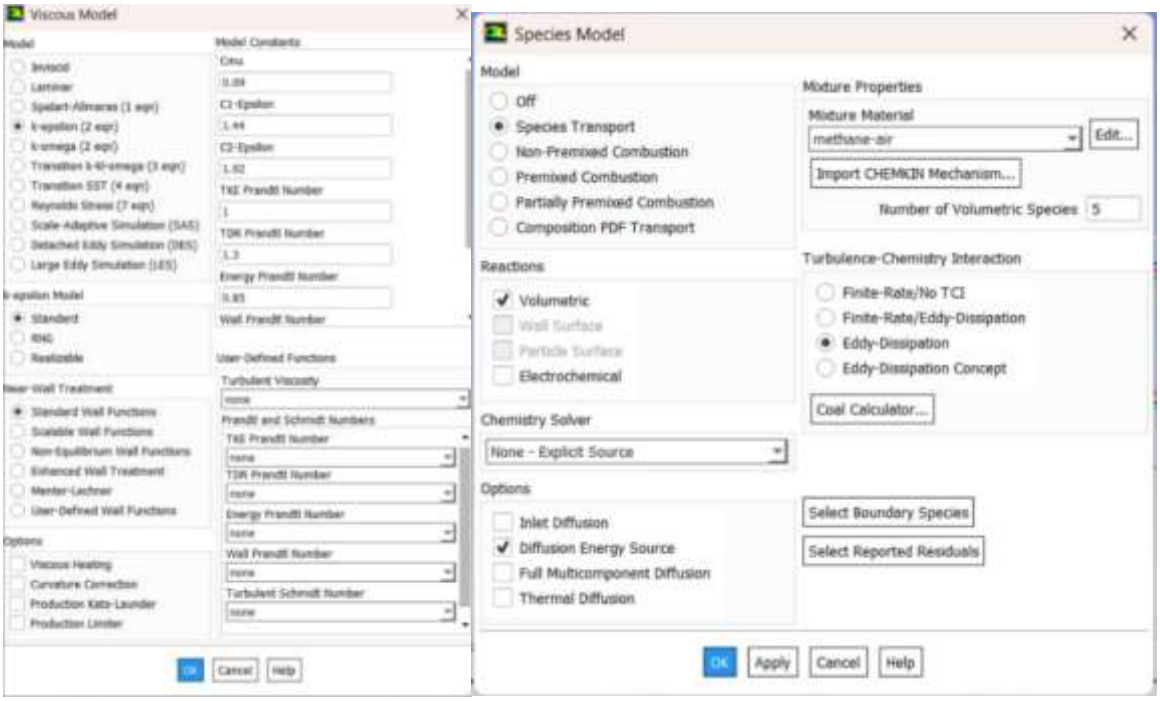

(a) (b)

Figure 2.10 Setup in RANS model (a) and species transport (b)

After selecting the appropriate model for the simulation process, the next step is to set up the boundary conditions. During the mesh generation process, the two inlets of the dual nozzle model have been defined, including Inlet 1 and Inlet 2:

- Inlet 1 corresponds to the air nozzle with the following settings:

  + Boundary type is set as velocity inlet.

  + Velocity is specified according to experimental conditions for the simulation cases.

  + Temperature is set at 300 K, which is the normalized initial value before any heat source from combustion reactions occurs.

  + The gas composition is air; since the focus is on simulating the combustion process, only the oxygen (O2) component is considered with a mass fraction set to 0.23.

- Inlet 2 corresponds to the fuel nozzle with the following settings:

  + Boundary type is velocity inlet.

  + Velocity is specified according to experimental conditions for the simulation cases.

  + Temperature is set the same as Inlet 1.

+ The gas component is the fuel methane (CH4), since this inlet is purely fuel, the mass fraction is set to 1.

After setting the boundary conditions, the next step is to establish the convergence criteria for the problem. The convergence criterion represents the allowable error threshold and reflects the accuracy of the simulation. Additionally, before starting the simulation, the choice of algorithm and interpolation method must be made. Selecting the appropriate algorithm and interpolation method is crucial to ensure the stability and accuracy of the results.

In this simulation, the SIMPLE algorithm is chosen. This is a pressure-velocity coupling algorithm used to solve the Navier–Stokes equations for incompressible flow. The algorithm works by initially predicting the pressure, solving the velocity equations to calculate and correct the pressure, and updating the velocity accordingly. This approach ensures stability and good convergence speed for the problem and is widely used in RANS models. Besides the solver algorithm, the simulation employs the Standard interpolation method to interpolate pressure values at the mesh cells. When combined with the SIMPLE algorithm, this method helps guarantee the accuracy and stability of the solution process.

2.4.2. Setup in the LES model

Large Eddy Simulation (LES) is a turbulence simulation method that provides higher accuracy compared to the conventional RANS models. LES does not perform a full Reynolds averaging like RANS; instead, it directly solves the large vortex structures (eddies), which are the main components influencing the transport of momentum, heat, and mass within the flow. Smaller eddies, which are less dependent on geometry and boundary conditions, are modeled indirectly through subgrid-scale turbulence models [7].

The main characteristics of LES include:

- LES directly solves the large turbulent structures that vary in time and space, therefore LES is always a transient model.
- It preserves the physical reality of the turbulence process, resulting in more accurate outcomes than RANS, especially in regions with strong variations such as flow separation zones, mixing regions, and combustion reactions.
- The computational cost is higher than RANS but significantly lower than DNS (Direct Numerical Simulation), making it suitable for problems requiring detailed description of flow structures.

However, LES has some limitations as it focuses on directly resolving the large eddies that vary strongly over time, thus the problem must be solved in a transient (time-dependent) manner. When LES is enabled, the solver settings automatically switch to transient mode, which results in significantly increased computational resources and simulation time. To enable a more accurate comparison with previous studies on the pulsed injection mode, LES simulation of the continuous injection mode under non-reacting conditions will be conducted.

In the non-reacting LES model, the Species Transport model is still used, but since this simulates the mixing process between air and fuel without combustion, the Volumetric Reactions option must be disabled. This option in the Species Transport model activates chemical reactions occurring within the flow volume. When enabled, the software solves the chemical reaction equations based on declared mechanisms, calculating combustion products, reaction rates, and heat release.

Therefore, when setting up the non-reacting LES model, Volumetric Reactions should be turned off to ensure the model only simulates the mixing and mass distribution process without chemical reactions. This significantly reduces computational cost as it avoids solving energy and reaction rate equations, optimizing computational efficiency.

Additionally, when enabling LES, selecting one of the Subgrid-Scale (SGS) models is mandatory. LES resolves large turbulent structures directly, but smaller eddies below the grid resolution cannot be accurately resolved due to mesh limitations. Hence, an SGS model is required to approximate the effects of these smaller eddies on the flow dynamics, ensuring completeness and accuracy of the simulation equations.

The SGS model will be set using the WALE method, which is suitable for accurately simulating turbulence near walls and in the region around the secondary disk.

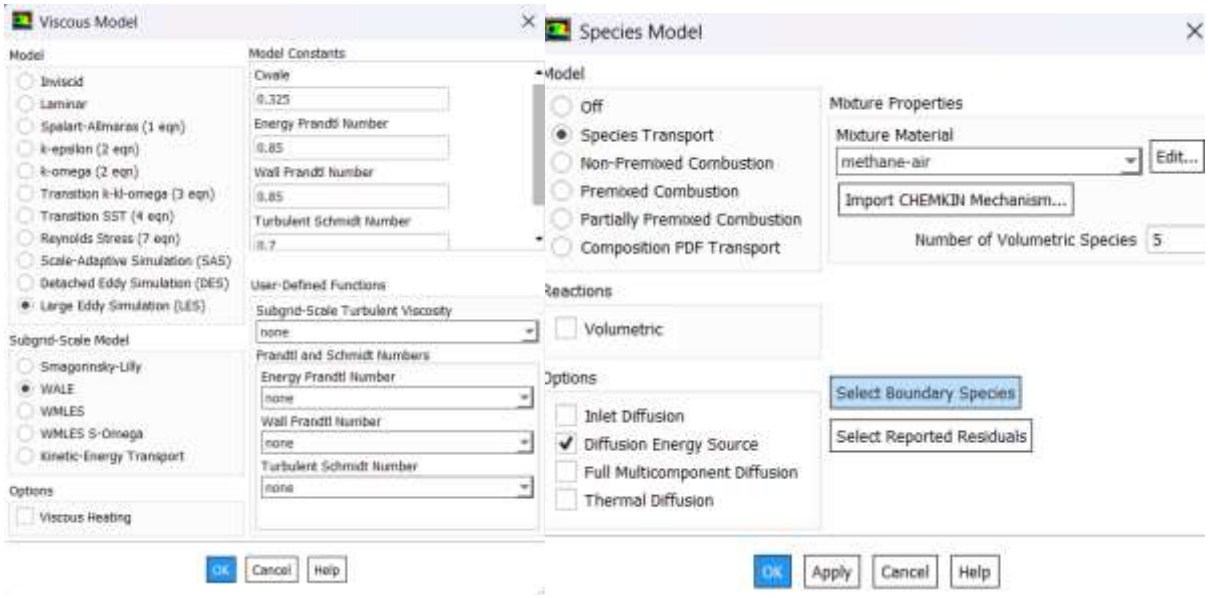

(a) (b)

Figure 2.11 Setup in the LES model (a) and species transport (b)

After selecting the appropriate model for the LES simulation, the next step is to set up the boundary conditions. These boundary conditions are established similarly to those used in the RANS model setup. Additionally, due to the high accuracy requirements in simulating the development and interaction of large turbulent structures over time in the LES model, the Coupled algorithm is chosen. This algorithm solves the momentum (velocity) and pressure equations simultaneously, ensuring a strong coupling between the velocity and pressure fields, thereby enhancing the stability and accuracy of the model at each time step.

2.5. Turbulence model analysis

After constructing the geometric model, setting up the mesh and appropriate boundary conditions, combined with computational algorithms and interpolation methods, the problem was simulated using ANSYS Fluent software. The simulation process aims to investigate the characteristics of the jet flow in three-dimensional space, focusing on factors affecting the development of the mixing zone, the propagation velocity of the jets, as well as the effects of the primary baffle disk and the velocity ratio between the fuel and air streams on flow characteristics and mixing efficiency.

The simulation results are presented in the form of velocity, temperature fields, and species concentration of CO2 produced from the combustion of Methane (CH4) an.

Equation of combustion reaction between two substances:

$$CH_4 + 2O_2 \rightarrow CO_2 + 2H_2O$$

From this, the influence of parameters such as the inlet velocity of air and fuel, as well as the effect of the primary baffle disk in the continuous injection case compared to the pulsed injection of the twin nozzle, on the development of the spray region can be evaluated. In addition, some comparisons between different velocity modes are conducted to indicate trends and optimize injection conditions.

When constructing simulations related to the combustion process, accurate setup of the energy equation and species transport plays a crucial role in correctly representing the physical nature of the chemical reaction process. The relevant equations are as follows:

The energy equation in Fluent describes the conservation of energy within the system. During combustion simulation, the heat generated by chemical reactions and the heat due to species diffusion play important roles in determining temperature distribution and combustion efficiency [7], and is expressed as follows:

$$\frac{\partial(\rho h)}{\partial t} + \nabla \cdot (\rho \vec{v} h) = \nabla \cdot (k_{\text{eff}} \nabla T) + S_h \quad (1.9)$$

Where:

ρ : Fluid density

h : Enthalpy (Total heat capacity)

$\vec{v}$: Velocity vector

k_{eff} : Thermal conductivity coefficient

T : Temperature

S_h : Energy source includes heat from chemical reactions, radiation heat, species diffusion heat, and viscous friction heat

Species Transport Equation Used to describe the change in mass fraction of each component in the flow. [7]

$$frac\partial(\rho Y_i)\partial t + \nabla \cdot (\rho \vec{v} Y_i) = -\nabla \cdot \vec{J}_i + R_i + S_i \quad (1.10)$$

Where:

Y_i : Mass fraction of the component i

$\vec{J}_i$: Diffusive flux of the component i

R_i : Reaction rate of formation or consumption of the component i

S_i : Additional source

CHAPTER 3: SIMULATION RESULT ANALYSIS

3.1. Simulation results Re_a = 1000

3.1.1. Case 1: V_a = 1.5 m/s and V_j =1 m/s

Residuals plot results:

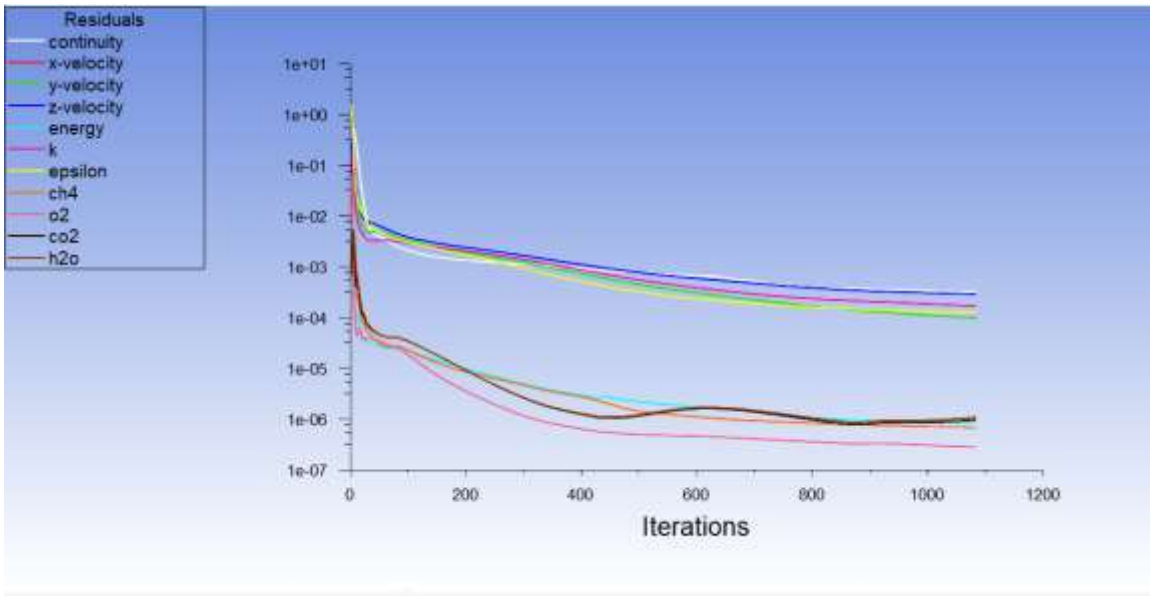

Figure 3.1 Residuals graph in the case V_a = 1.5 m/s và V_j =1 m/s

First, the residuals graph is used to monitor the convergence of the calculation process. The x-axis of the graph represents the iteration steps for the calculation; in this case, it approaches nearly 1100 steps. The y-axis represents the residual values, also known as convergence errors; the smaller the residual, the higher the accuracy of the problem. From the graph shown, it is observed that during the iterations from 0 to 500, all residual curves decrease rapidly, but from step 500 onwards, the curves decrease more slowly and tend to stabilize. In the graph, the continuity and velocity residuals in the x, y, z directions, as well as epsilon, run around the order of 10^(-3). Although this does not reach the optimal value, it is still acceptable for a complex RANS problem with chemical reactions.

However, the residuals for the energy equation and the mass transport equations of the reacting species (CH4, O2, CO2, H2O) have dropped to values between 10^(-5) and 10^(-6), indicating good convergence and reliability of the combustion model. The species and combustion products are simulated accurately. Furthermore, the curves for combustion products CO2 and H2O show some oscillations but remain small, within residual values from 10^(-5) to 10^(-6). This may be because during the combustion

simulation, these products are not generated immediately but evolve with the development of the reaction zone or flame region. Therefore, the CO2 and H2O residuals are not as stable early on compared to those of CH4 and O2.

To clearly visualize the mixing between the air stream and the fuel stream, velocity streamlines are displayed. These streamlines represent the flow direction and velocity magnitude of air and fuel at each location within the computational domain. As shown in the Figure 3.2 below, the red lines indicate the highest velocity of the air stream at 1.6 m/s, while the orange-yellow lines at the outlet of the fuel nozzle have velocities ranging from 1 m/s to 1.2 m/s. It can be observed that the velocity lines of the fuel stream slow down gradually and reduce to zero right at the contact with the secondary baffle disk.

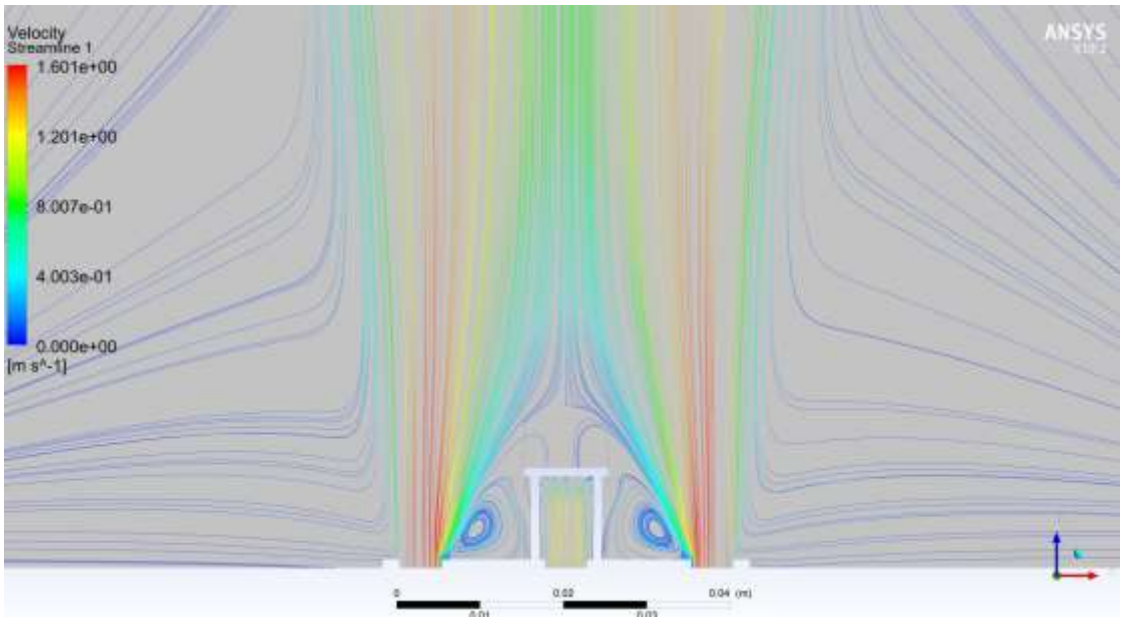

Figure 3.2 The velocity streamlines field in the case Va = 1.5 m/s và Vj =1 m/s

As shown in the Figure 3.2, when the air stream is sprayed out at a high velocity, the central pressure of the nozzle also increases. According to Bernoulli's principle, an increase in velocity leads to a decrease in static pressure at the edges of the nozzle exit. The region between the fuel nozzle and the air nozzle shown in the Figure 3.2 corresponds to this low-pressure zone. By this principle, air flows from areas of higher pressure to lower pressure, creating a suction effect that forms a swirling air flow. This effect accelerates the mixing process between air and fuel.

Combined with the secondary baffle disk, which creates a reaction force zone, this reduces the velocity of the fuel stream as it hits the disk. With the fuel velocity reduced, when the fuel flow impacts the rear side of the secondary baffle disk, a blocking

region forms in front of the fuel nozzle exit, simultaneously creating a high-pressure zone in front of the baffle. This pressure region drives air from outside to move into the intermediate zone where the fuel is sprayed, generating a suction vortex. However, due to the low velocity of the fuel stream, the momentum of the fuel jet is not strong enough to pass through the secondary baffle disk. Because the energy of the flow is weak, observation of the Figure 3.2 shows that a vortex is about to form on the secondary baffle disk.

Because of this, when the fuel velocity is low, the flame zone forms very close to the nozzle exit and mainly concentrates on the upper part of the secondary baffle disk. Due to the low fuel velocity, the fuel stream lacks sufficient kinetic energy to penetrate the air layer surrounding the baffle disk and its structure, causing the fuel region to have difficulty spreading upward. This limits the flame thickness. According to the temperature field distribution shown in the Figure 3.3, the combustion process tends to cling closely to the baffle disk, resulting in limited heat propagation and reduced heat dissipation efficiency, causing a short and localized temperature field.

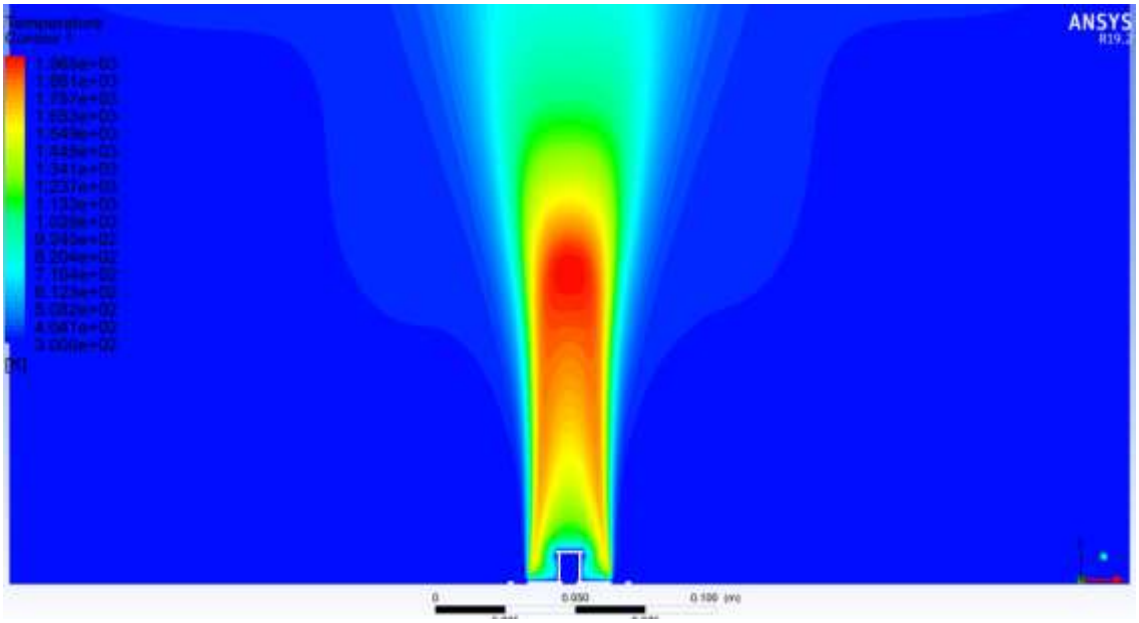

Figure 3.3 Temperature field distribution in the case Va = 1.5 m/s và Vj =1 m/s

Based on the temperature field distribution from the simulation Figure 3.3, the trend of the concentration field distribution can be inferred. During the injection, mixing, and combustion process between oxygen (O_2) and methane (CH_4) fuel, the combustion products generated are CO_2 and H_2O. Where the combustion reaction occurs efficiently, there is a high heat generation zone, which also corresponds to the highest concentration of CO_2, indicating that the fuel is completely oxidized.

However, in this case, due to the low fuel velocity, the combustion reaction takes place within a small region, as shown by the temperature field. Similarly, the CO_2 concentration reaches its maximum where the heat generation is highest, and the concentration gradually decreases along with the temperature field. This is confirmed by the CO_2 concentration distribution field shown in the Figure 3.4.

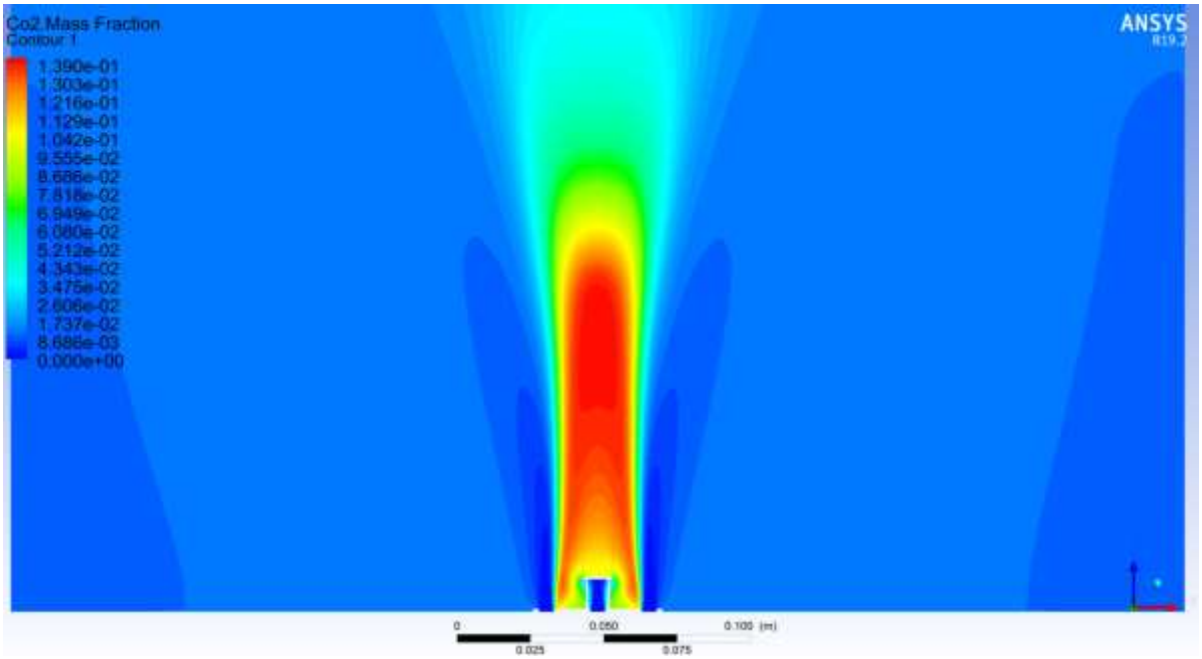

Figure 3.4 CO_2 concentration distribution in the case Va = 1.5 m/s và Vj =1 m/s

3.1.2. Case 2: V_a = 1.5 m/s and V_j =2.5 m/s

Residuals plot results:

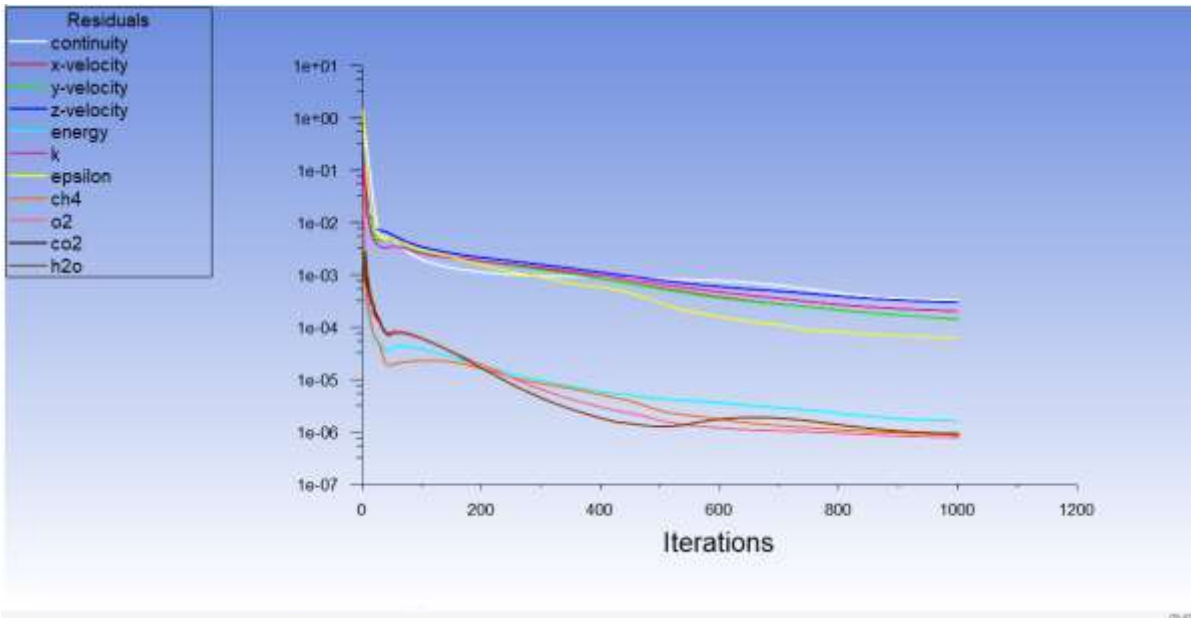

Figure 3.5 Residuals graph in the case V_a = 1.5 m/s và V_j =2.5 m/s

Basically, the continuity line, the velocity line in the x, y, z directions and epsilon, the energy lines, the mass transport equation lines of the substances in the reaction (CH4, O2, CO2, H2O) are all shown the same as in case 1, the only difference is that in this case the number of steps is 1000, less than case 1.

Results of the velocity streamlines field:

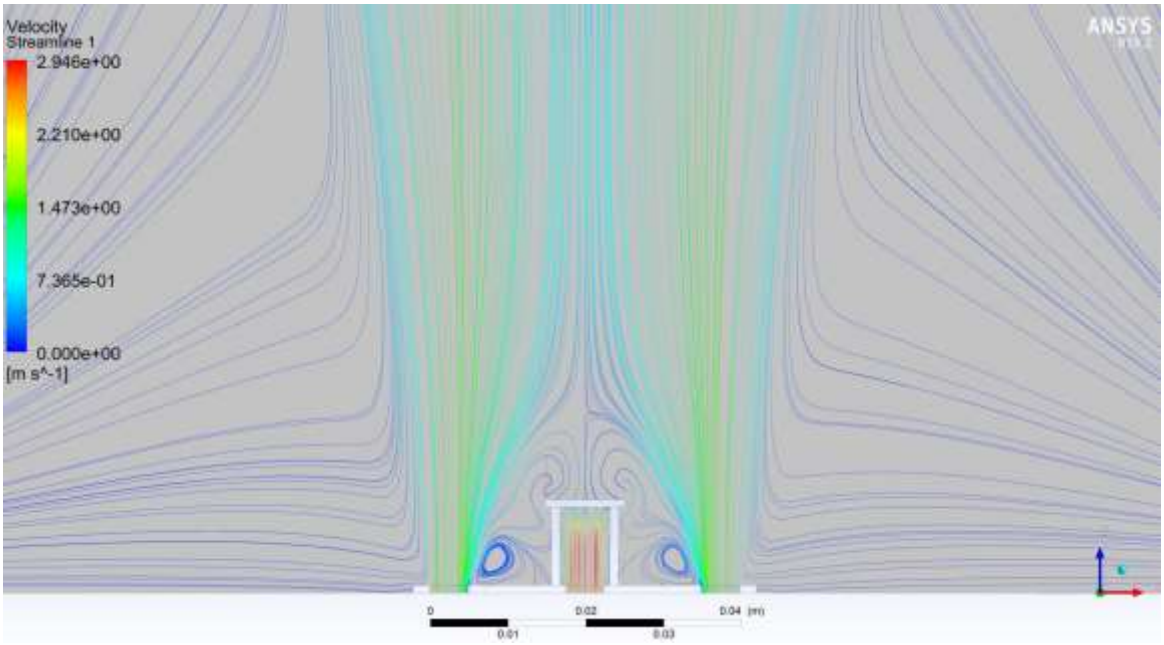

Figure 3.6 The velocity streamlines field in the case V_a = 1.5 m/s và V_j =2.5 m/s

In this case, the air velocity remains constant at V_a = 1.5m/s, while the fuel velocity increases to V_j = 2.5 m/s, as calculated by the software and represented by the red line, which gradually decreases and approaches zero at the contact with the baffle plate.

At this point, when the fuel velocity is higher and the momentum of the fuel jet is stronger, despite the secondary baffle plate still exerting an influence, its effect is less significant. Although it can still block the fuel flow at the center of the plate, the strong momentum of the jet tends to deflect the flow towards the edge of the baffle due to the pressure at the edge and the pressure on the upper surface of the plate. This creates a flow separation phenomenon and a small vortex region on the surface of the baffle.

This vortex region helps to enhance the mixing between the air and fuel streams, thereby increasing the mixing efficiency and improving the combustion performance. Furthermore, with the higher fuel velocity, although affected by the secondary baffle, the kinetic energy of the fuel stream is greater than in the first case, allowing the fuel jet to be pushed further away from the nozzle. This increases the combustion efficiency and

causes the high-temperature zone to expand horizontally, indicating better heat dispersion. This is demonstrated by the temperature field distribution Figure 3.7 below.

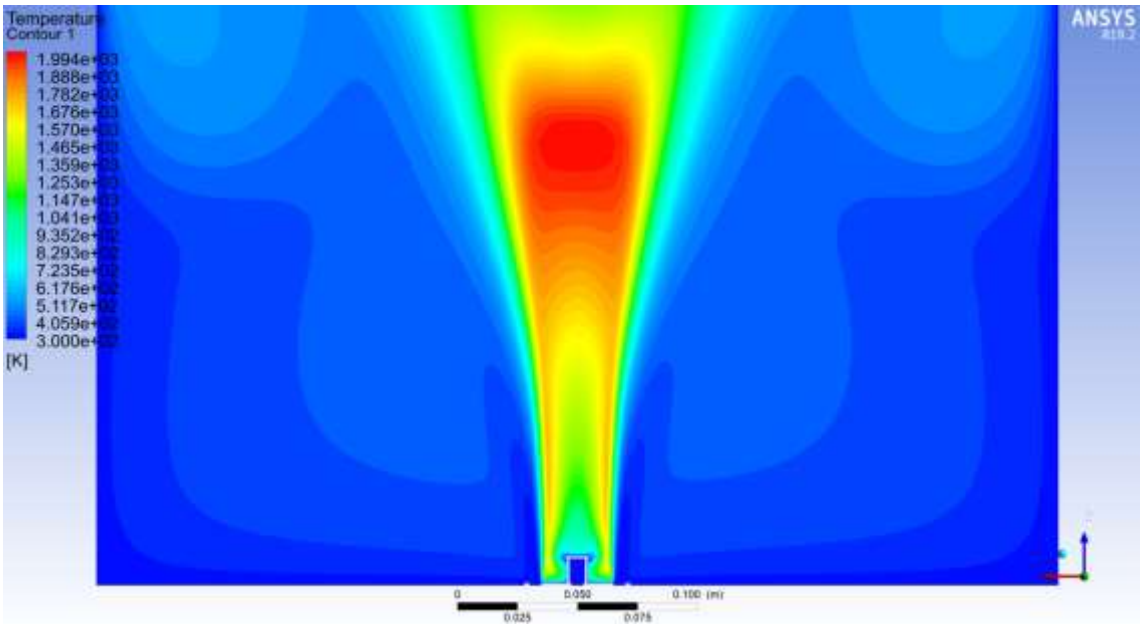

Figure 3.7 Temperature field distribution in the case Va = 1.5 m/s và Vj =2.5 m/s

The temperature distribution field in this case is wide and the temperature zone is wide and extended to both sides, indicating that the mixing and reaction process in this case is also extended to both sides, which contributes to the distribution of CO_2 over a wider area, increasing the combustion efficiency. Combined with the vortex generated from the blocking disc and the momentum difference between the two air and fuel streams, it helps to diffuse CO_2 out of the reaction core area.

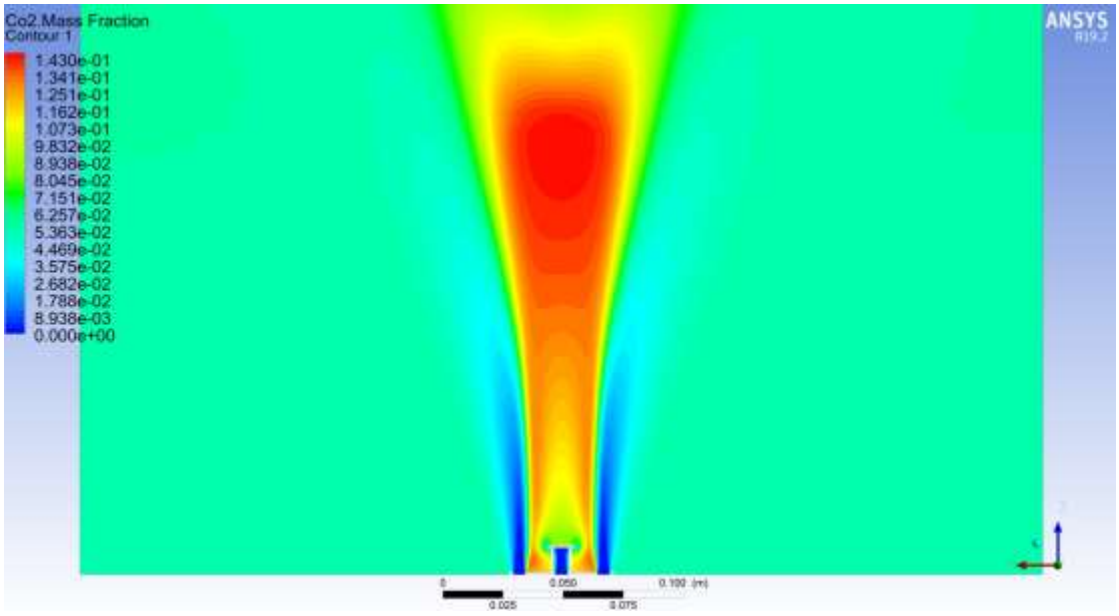

Figure 3.8 CO_2 concentration distribution in the case V_a = 1.5 m/s và V_j =2.5 m/s

3.1.3. Case 3: V_a = 1.5 m/s and V_j = 5 m/s

Residuals plot results:

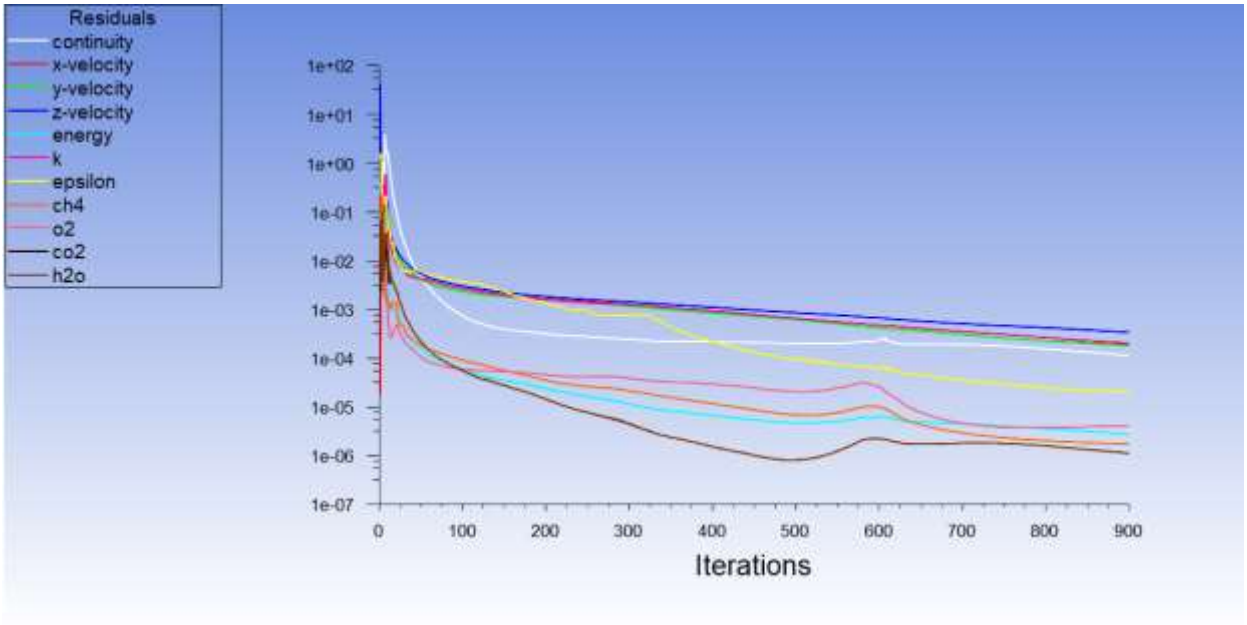

Figure 3.9 Residuals graph in the case V_a = 1.5 m/s và V_j = 5 m/s

In the case of V_a = 1.5 m/s and V_j = 5 m/s, the fuel flow velocity is increased and is significantly higher than in the previous cases. The purpose of this velocity increase is to investigate the influence of the jet momentum on the mixing process between fuel and air, as well as the impact on the formation of the vortex field. To be able to analyze these effects, see the velocity streamline field results below.

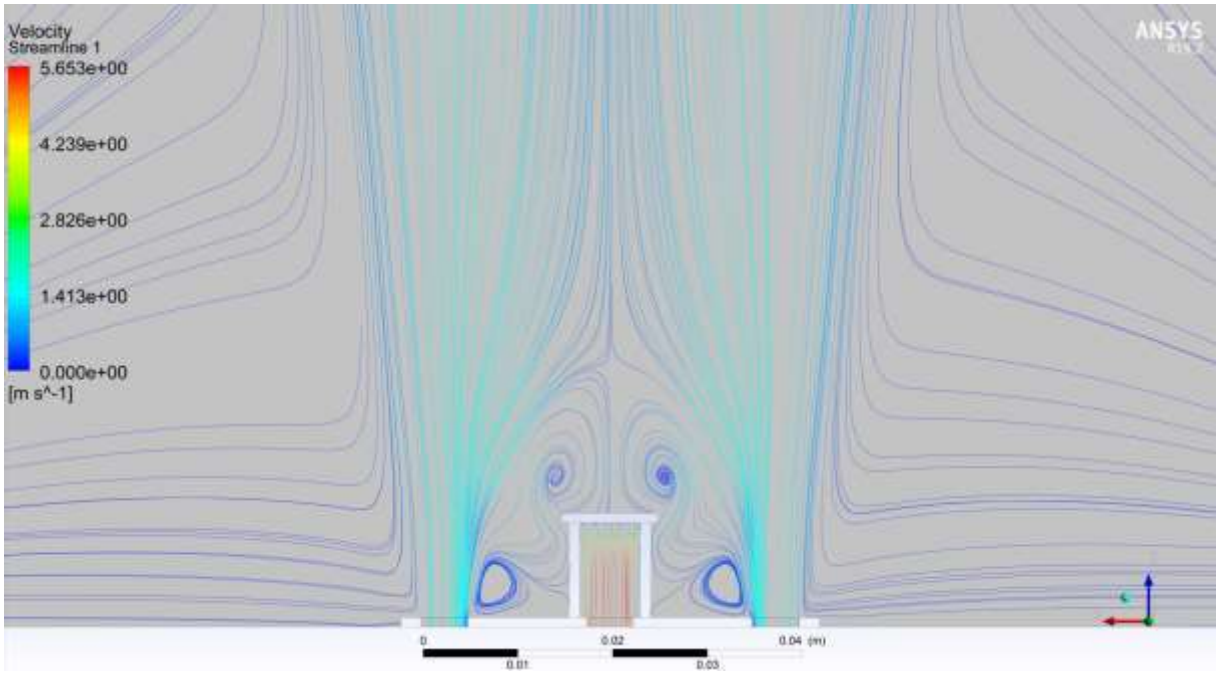

Figure 3.10 The velocity streamlines field in the case V_a = 1.5 m/s và V_j = 5 m/s

In the case where the fuel velocity V_j = 5 m/s , as shown in the Figure 3.10, there are four vortex flows: two located between the air nozzle and the fuel nozzle, and two others appearing above the secondary baffle plate. According to the velocity streamline distribution in the Figure 3.10, these vortex regions are clearly more developed in both size and intensity.

At this stage, the fuel jet has very high kinetic energy. When the fuel stream reaches the edge of the secondary baffle, it causes a velocity and pressure difference between the fuel jet at the baffle edge and the top surface of the plate. This generates strong turbulence and vortices around the top surface of the baffle, enhancing the mixing efficiency.

Meanwhile, the portion of the flow blocked by the baffle is pushed aside by the high-velocity fuel stream. As a result, the air encountering the secondary baffle is forced to move laterally to both sides, spreading widely.

The combination of suction from the low-pressure zone and lateral pushing caused by the baffle creates a strong airflow motion from both sides of the jet, helping to distribute the air more evenly and extensively in the reaction zone. This enhances the mixing process between the fuel and air, resulting in a more efficient combustion reaction, as shown in the temperature field below.

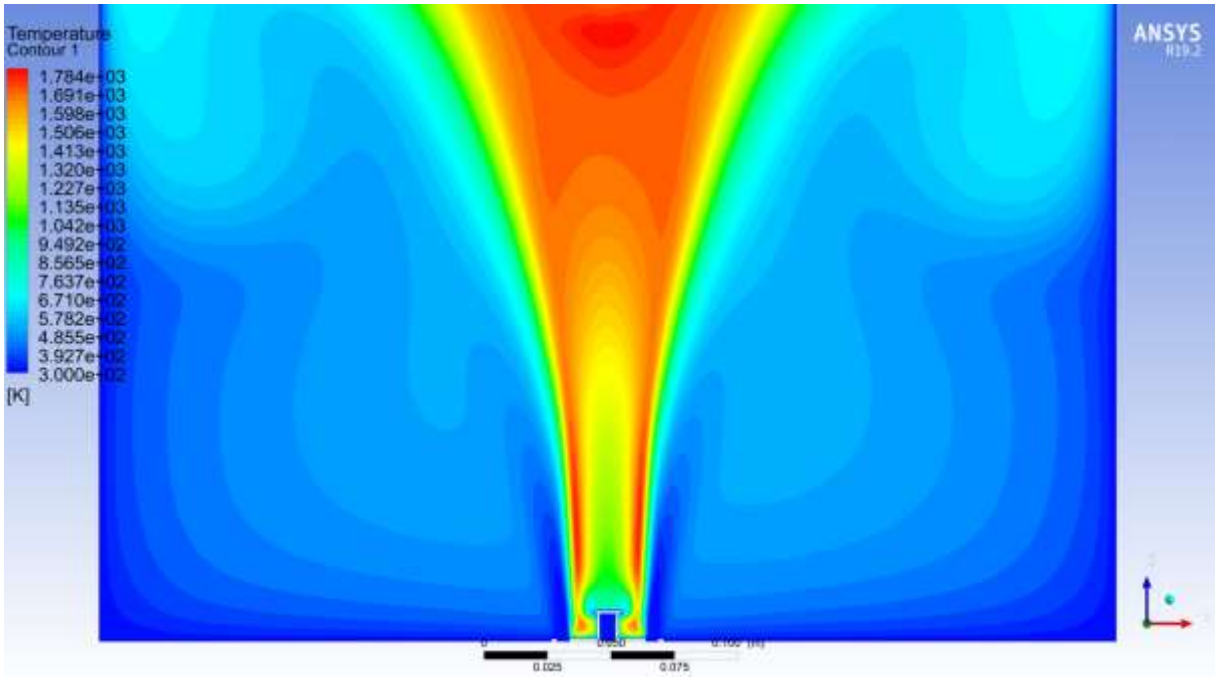

Figure 3.11 Temperature field distribution in the case V_a = 1.5 m/s và V_j = 5 m/s

The temperature field clearly indicates the affected region and shows a strong concentration of heat distribution along the main axis of the jet, forming a high-temperature cone extending from the nozzle tip to the upper region. Additionally, due to the presence of vortices at the edges of the baffle plate, some fuel is dragged to both sides, creating an expanded combustion zone in the horizontal direction. At these locations, medium-high temperature bands spreading horizontally can be observed, demonstrating better mixing efficiency between fuel and air compared to cases one and two.

Based on the temperature field obtained from the simulation, the CO_2 concentration field can be predicted. Essentially, the highest temperature zone corresponds to the highest CO_2 concentration area, with the combustion products spreading primarily along the vertical axis (Z), while also expanding laterally, similar to the temperature distribution.

Looking at the overall comparison among the three simulation cases, it can be seen that the case with V_a = 1.5 m/s and V_j = 5 m/s, where the fuel velocity is high, exhibits the largest combustion coverage and the widest CO_2 concentration distribution within the domain. This indicates that increasing the fuel velocity helps improve the mixing capability with air, promoting the combustion process and enhancing the production efficiency of combustion products

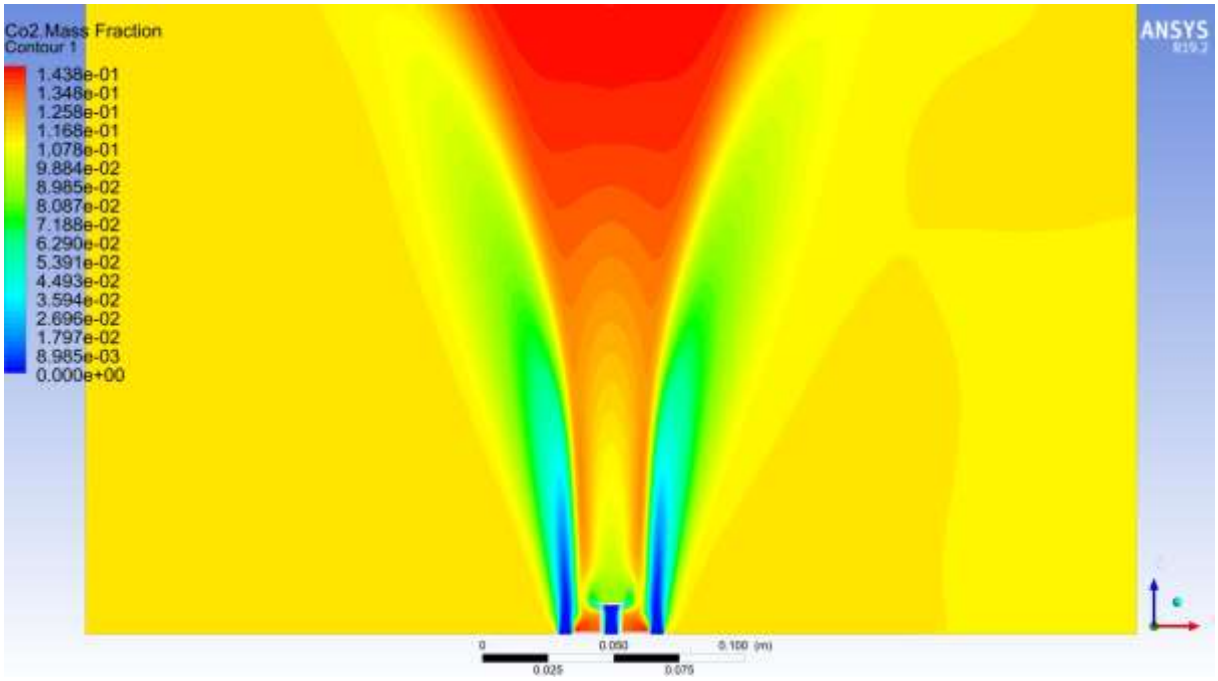

Figure 3.12 CO_2 concentration distribution in the case V_a = 1.5 m/s và V_j = 5 m/s

3.2. Simulation results Re_a = 5000

3.2.1. Case 4: V_a = 7.5 m/s and V_j = 1 m/s

Based on the Figure 3.13 below, it can be observed that within the iteration range from 0 to 200, all residual curves drop rapidly. However, from iteration 200 onwards, the curves decrease more slowly and tend to stabilize. In the graph, the residuals for continuity and velocity components in the x, y, and z directions, as well as epsilon, fall within the range of 10^(-3). The residuals for energy and for the mass transport equations of species involved in the reaction (CH_4 , O_2 , CO_2 , H_2 O) have dropped to values between 10^(-5) and 10^(-7). Overall, the residuals graph in the case of Reynolds number 5000 is similar to that of Reynolds number 1000, but the curves for CO_2 and H_2 O exhibit less fluctuation.

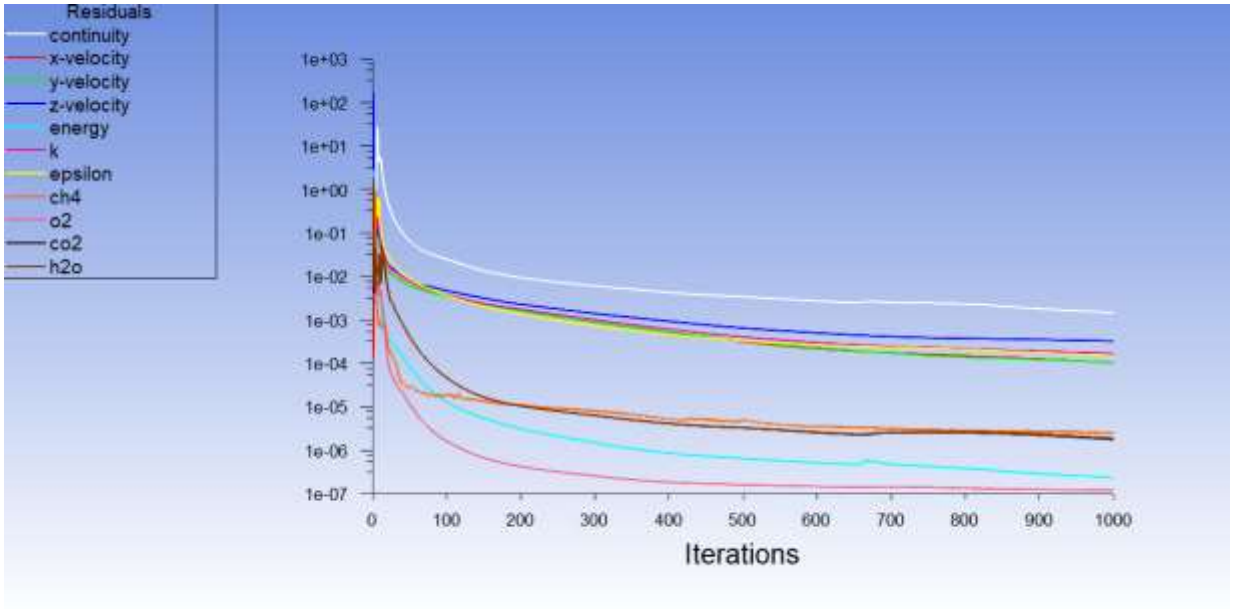

Figure 3.13 Residuals graph in the case V_a = 7.5 m/s và V_j = 1 m/s

After the convergence of the simulation process was confirmed through the Residuals graph, the results were exported, including the velocity streamlines, temperature field distribution, and CO_2 concentration generated from the combustion process.

Results of the velocity streamlines field:

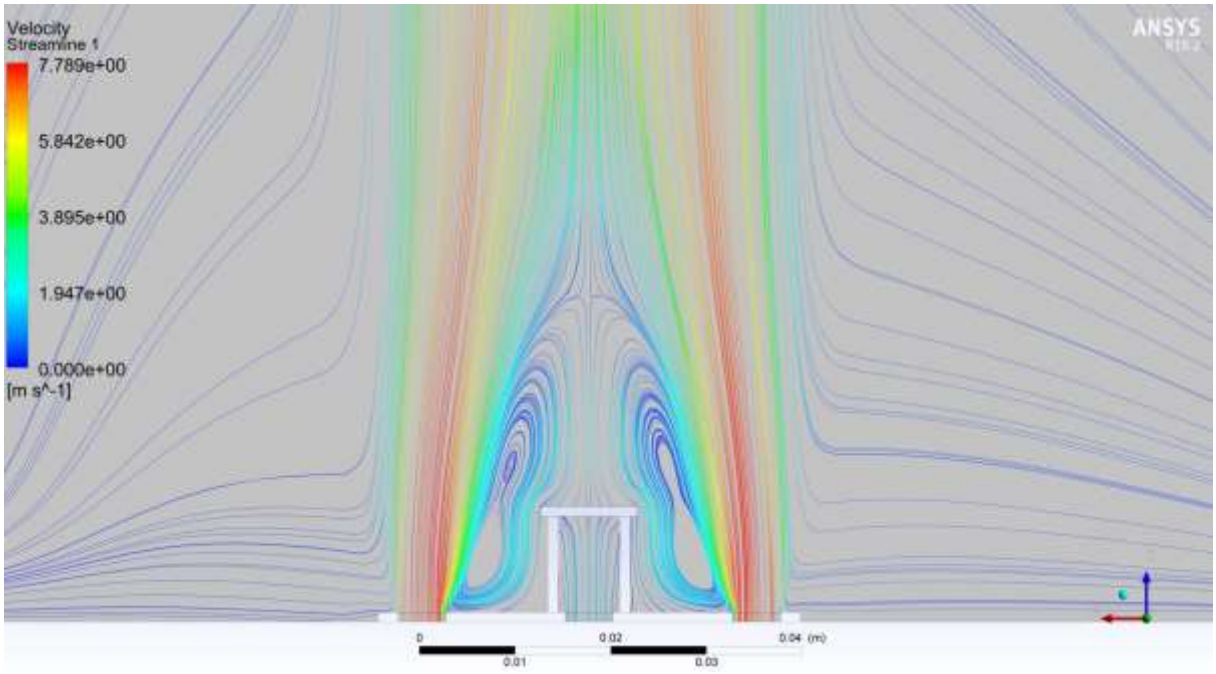

Figure 3.14 The velocity streamlines field in the case V_a = 7.5 m/s và V_j = 1 m/s

In the case where the velocity of the air stream V_a = 7.5 m/s is significantly higher than that of the fuel stream, the pressure difference between the air jet being injected and the ambient pressure near the nozzle exit becomes substantial. This leads to a noticeable impact on the flow structure, as can be observed in the velocity streamline field. The pressure difference induces a large vortex that extends from the nozzle tip up to beyond the secondary bluff body. In this simulation, the fuel stream velocity is still low V_j = 1 m/s, and due to the influence of the strong vortex, the fuel is drawn outward to both sides, while also entraining surrounding air into the mixing region. This increases the mixing zone and enhances the combustion process.

Moreover, when the vortex has high intensity and the fuel velocity is low, the fuel is significantly affected by centrifugal forces and suction forces created by the vortex. Under these conditions, the fuel lacks sufficient momentum to penetrate upward or propagate outward, and instead is pulled back into the central vortex region just behind the secondary bluff body. This phenomenon is more clearly illustrated in the temperature field shown below.

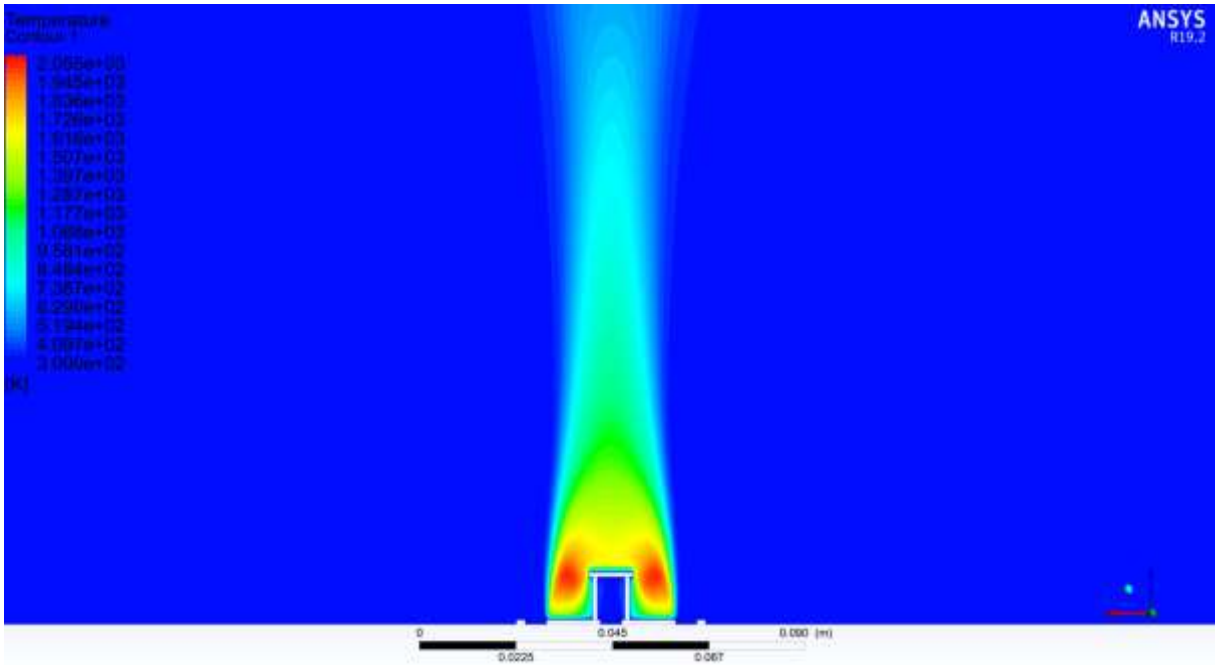

Figure 3.15 Temperature field distribution in the case V_a = 7.5 m/s và V_j = 1 m/s

According to the temperature field distribution, the highest temperature occurs within the vortex region. This indicates that the flame tends to contract and concentrate near the secondary bluff body, as combustion mainly takes place in the vortex area where fuel and air are drawn in and retained, forming an effective mixing zone.

This can be explained by the fact that when the air velocity is significantly higher than the fuel velocity, a strong vortex is formed immediately downstream of the air nozzle and just behind the secondary bluff body, dominating the entire flow field in that region. Due to its low velocity, the fuel lacks sufficient momentum to escape this vortex. As a result, the fuel is trapped near the initial combustion zone, causing the combustion process to be concentrated in a localized lower region rather than being evenly distributed along the height of the Domain. As a result, this affects the combustion efficiency, emission levels, and flame stability across different configurations, thereby reducing the overall mixing effectiveness between air and fuel. This is especially evident in the region above the secondary bluff body, where the fuel is unable to overcome the strong vortex and spread uniformly along the vertical extent of the domain.

The CO_2 concentration field confirms this, as the region with the highest CO_2 concentration coincides with the high-temperature zone. The distribution pattern of CO_2 is nearly identical to that of the temperature field. The highest concentration region is

indicated by the red area, with a maximum CO_2 concentration value of 0.1415.

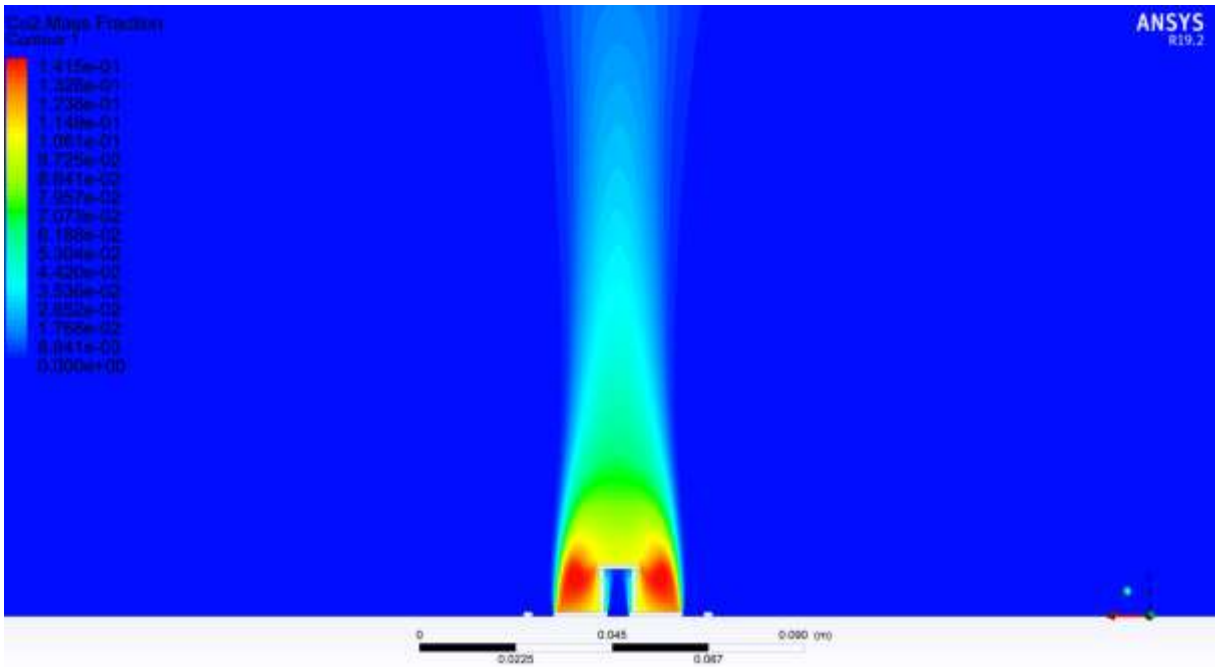

Figure 3.16 CO_2 concentration distribution in the case V_a = 7.5 m/s và V_j = 1 m/s

3.2.2. Case 5: V_a = 7.5 m/s and V_j = 2.5 m/s

Residuals Plot results:

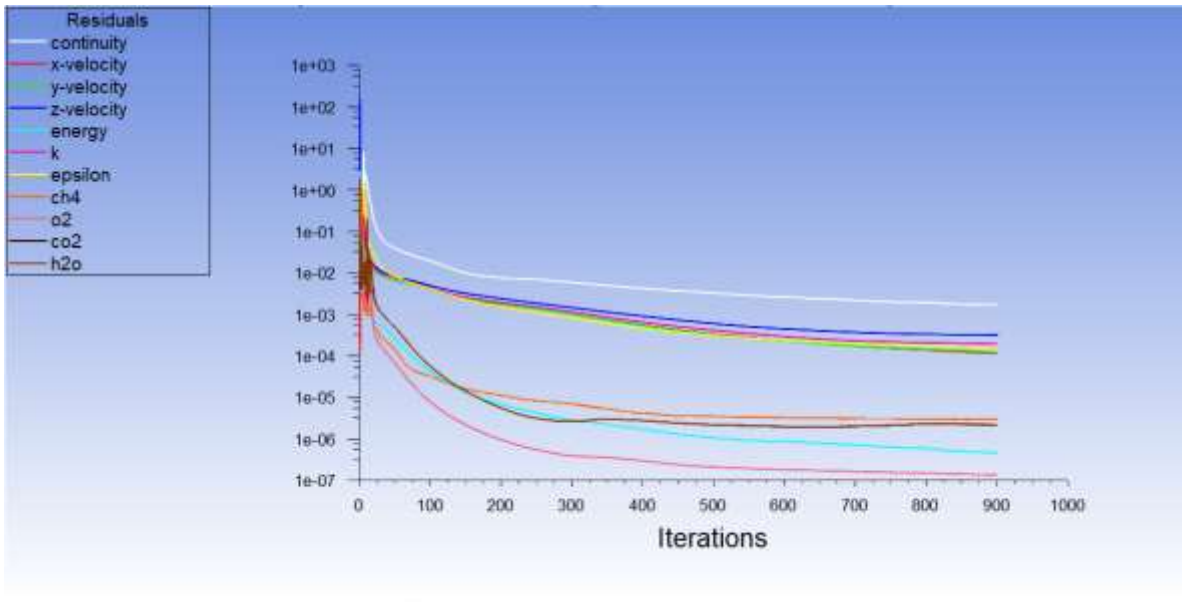

Figure 3.17 Residuals graph in case V_a = 7.5 m/s và V_j = 2.5 m/s

Results of the velocity streamlines field:

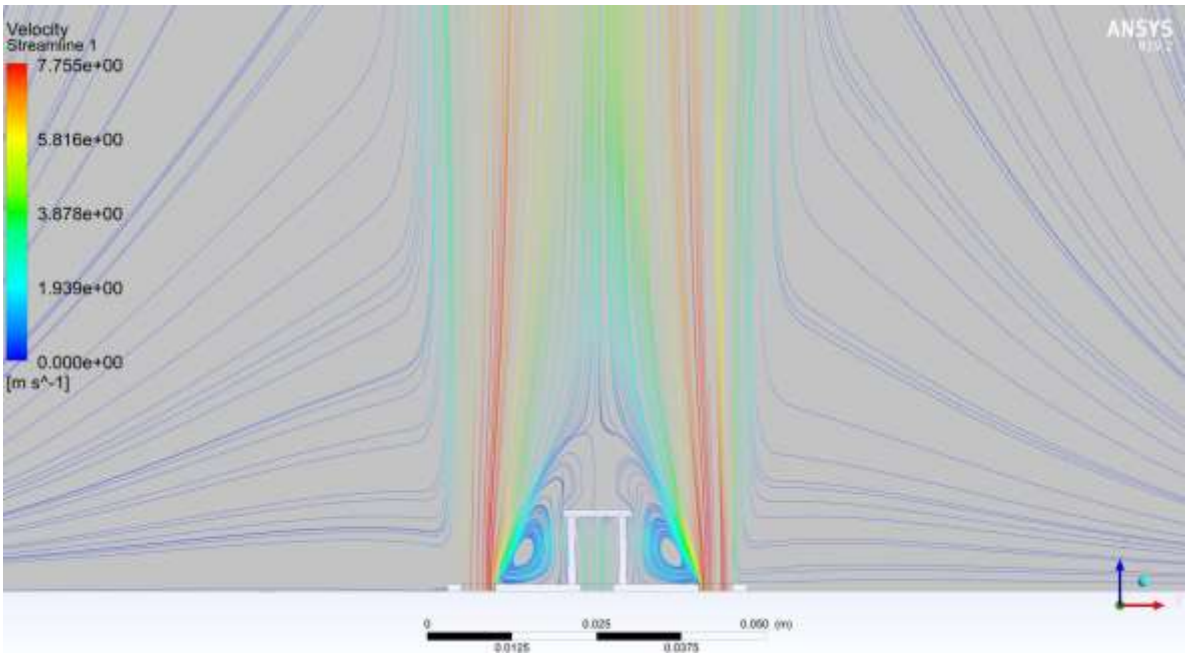

Figure 3.18 The velocity streamlines field in the case V_a = 7.5 m/s và V_j = 2.5 m/s

In this simulation case, the fuel jet velocity is increased to V_j = 2.5 m/s, resulting in changes in the velocity distribution field and the development of the vortex region. This is reflected in the streamline pattern, where the vortex region appears smaller compared to the case with a lower fuel velocity of V_j = 1 m/s. The increase in fuel velocity also means an increase in fuel jet momentum, which makes the fuel flow less susceptible to the influence of the vortex created by the pressure difference from the air jet.

However, since the air stream still has a higher velocity, the fuel flow is still affected to some extent. A portion of the fuel at the outer edge is pulled toward the vortex, while another portion escapes being completely entrained and flows from the edge of the secondary bluff body, penetrating and resisting the downward vortex generated by the air stream. This behavior will be further clarified through the temperature field distribution.

According to the temperature field shown below, it can be clearly observed that the temperature distribution or combustion zone in the case of V_j = 2.5 m/s is distinctly different from the simulation case with V_j = 1 m/s. Due to the higher momentum of the fuel jet, a portion of the flow initially passes the first bluff body and is partially affected by the air-induced vortex. At this stage, the fuel stream expands and mixes with the surrounding air, forming a large initial combustion region. However, as the fuel continues to pass beyond the secondary bluff body, it is subjected to the influence of the

high-speed air stream. Since the fuel momentum is not sufficiently strong, the further it rises, the narrower the combustion zone becomes. This behavior is visualized more clearly in the temperature contour presented below.

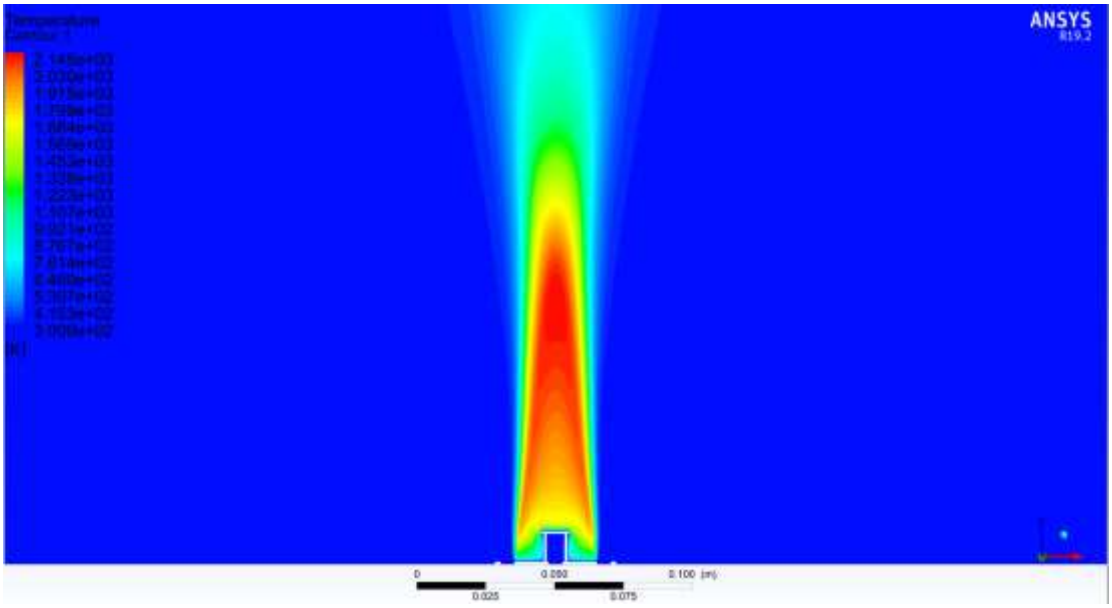

Figure 3.19 Temperature field distribution in the case V_a = 7.5 m/s và V_j = 2.5 m/s

The CO_2 concentration field clearly shows a well-defined distribution, where regions with the highest CO_2 concentrations correspond to areas of intense combustion as indicated by the high temperature field. The CO_2 concentration gradually decreases due to dilution with the surrounding air and the dissipation of thermal energy. In this simulation case, the maximum CO_2 concentration reaches a value of 0.1418.

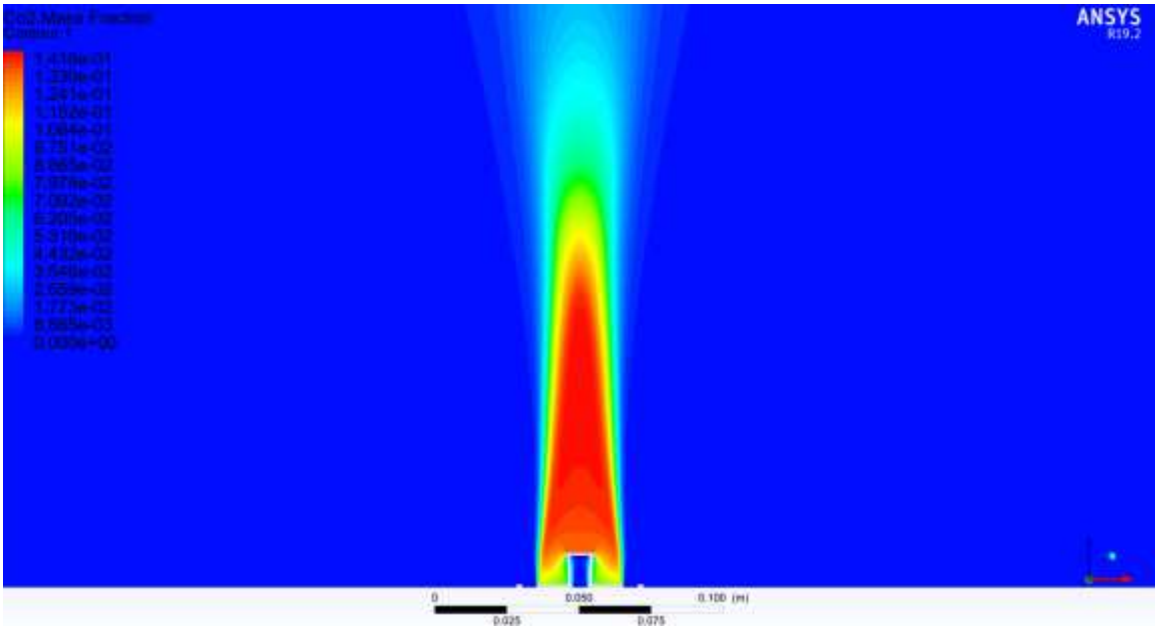

Figure 3.20 CO_2 concentration distribution in the case V_a = 7.5 m/s và V_j = 2.5 m/s

3.2.3. Case 6: V_a = 7.5 m/s and V_j = 5 m/s

Residuals plot results:

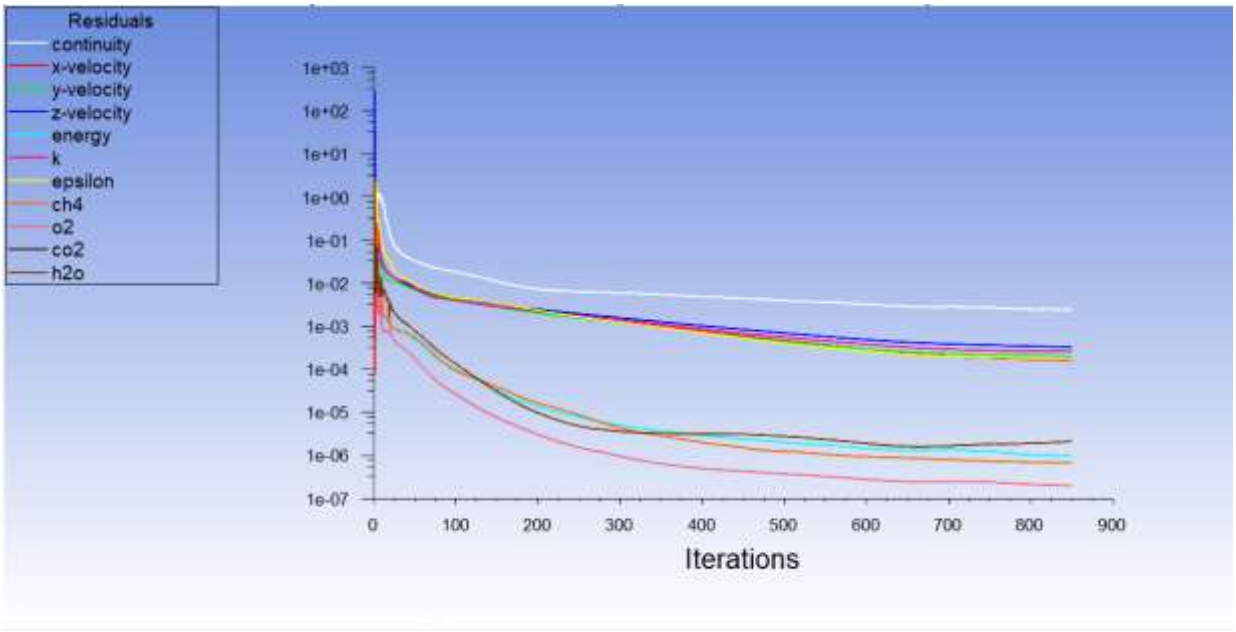

Figure 3.21 Residuals graph in the case V_a = 7.5 m/s và V_j = 5 m/s

Results of the velocity streamlines field:

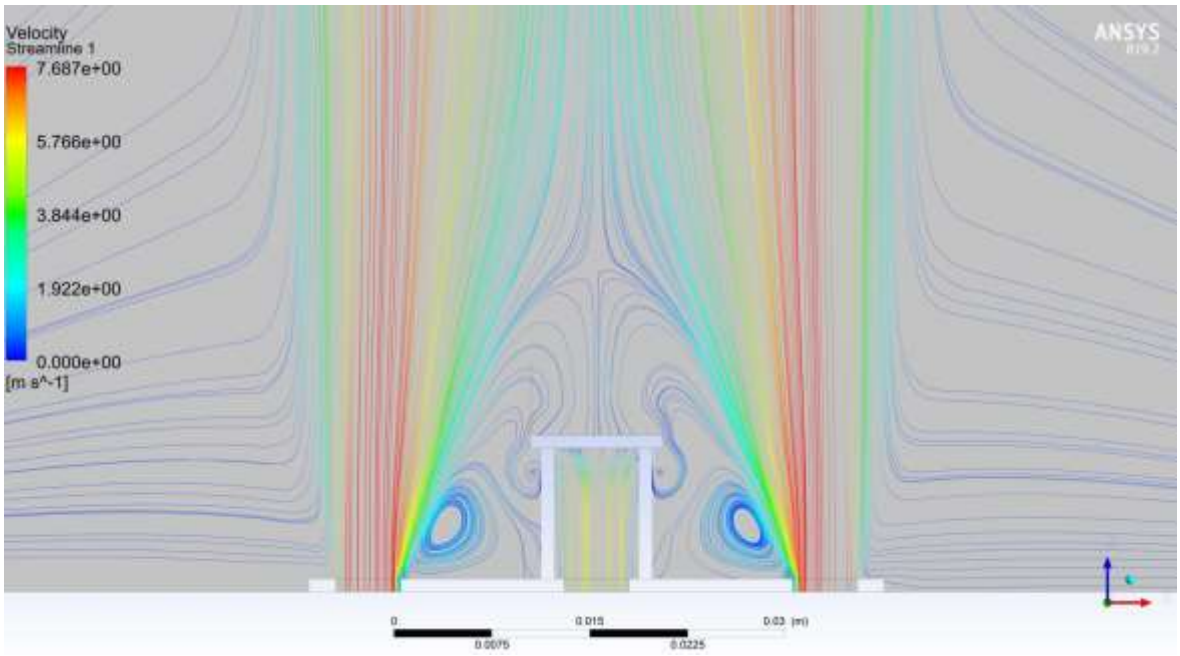

Figure 3.22 The velocity streamlines field in the case V_a = 7.5 m/s và V_j = 5 m/s

In this simulation case, the velocity of the fuel jet is V_j = 5m/s. As the fuel velocity increases, the momentum of the fuel stream also increases accordingly. This is most clearly demonstrated by the velocity streamline field results. Observing the

velocity streamline field reveals a significant difference in the case of V_j = 5 m/s compared to the previous cases with V_j =1 m/s and V_j = 2.5 m/ s, particularly in the region from the nozzle outlet to the secondary bluff body, where four distinct vortex regions appear. Among them, two vortices are located between the air and fuel jets, formed due to the high velocity of the air stream causing pressure differences that generate vortices. The other two vortices are located near the edges of the secondary bluff body, with one vortex directly behind the bluff body oriented toward the fuel nozzle inlet.

This phenomenon is the result of flow separation and recirculation occurring when the high-speed airflow interacts with the bluff body shape, which is the edge of the secondary disk. In this area, when the airflow passes through the narrow gap between the two disks (primary and secondary), and encounters a sudden change in cross-sectional area and flow direction, a local pressure difference appears. In front of the secondary disk, the pressure is relatively high, while the area behind it has lower pressure because the airflow separates from the surface. As a result, the airflow is pulled backward and forms recirculation vortex zones right behind the disk.

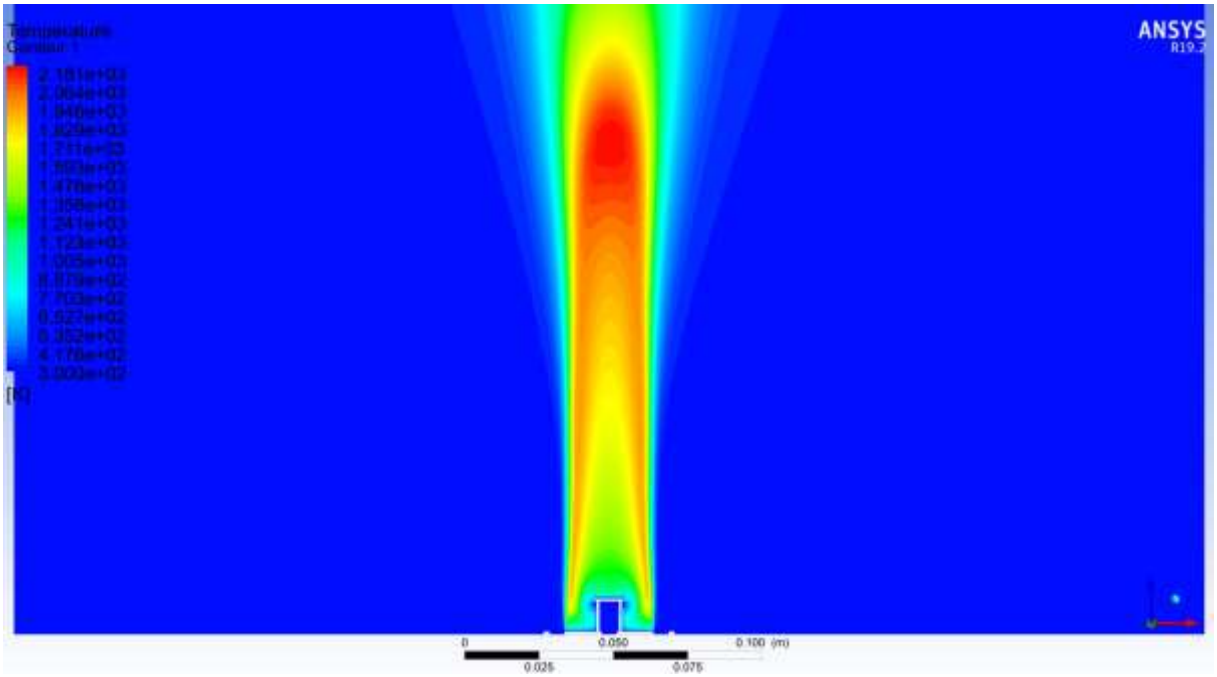

Figure 3.23 Temperature field distribution in the case V_a = 7.5 m/s và V_j = 5 m/s

The Figure 3.23 above represents the temperature field. Observation shows that the highest temperature in the field is 2181 K, and the high-temperature region is concentrated and uniform. This indicates that the fuel and air are well mixed, and the combustion reaction occurs evenly.

Due to the influence of the high velocity of the fuel jet, when the flow passes through the secondary bluff body, its momentum is still significantly preserved**.** As illustrated in the Figure 3.23, the combustion process in this case occurs at a location farther downstream compared to the previous two simulation cases. Since the energy is concentrated along the central axis, lateral heat dispersion is limited, leading to a reduced thermal spread to the surrounding environment.

CO_2 concentration field results:

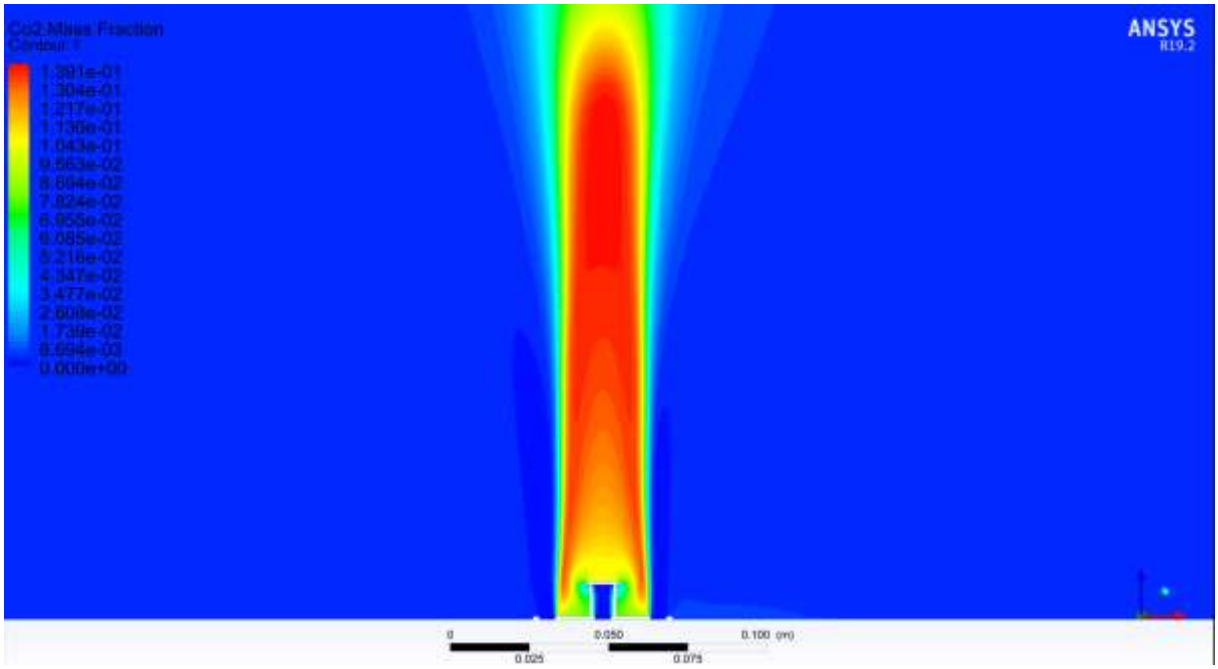

Figure 3.24 CO_2 concentration distribution in the case V_a = 7.5 m/s và V_j = 5 m/s

The simulation results of the CO_2 concentration field show that the maximum concentration reaches 0.139, represented by the red-colored region. Based on the temperature distribution results, it can be observed that regions with the highest CO_2 concentrations also correspond to areas of high temperature, indicating significant pollutant emissions. In contrast, areas with lower temperatures are also those with lower CO_2 concentrations.

3.3. Constructing and analyzing kinematic graphs based on velocity, temperature, and CO_2 concentration fields

Based on the simulation data, including the velocity, temperature, and CO_2 concentration fields at different fuel jet velocities and Reynolds numbers, ANSYS Fluent is used to plot the distribution graphs of velocity, temperature, and CO_2 concentration along the injector axis for the cases of Re_a = 1000 and Re_a = 5000, corresponding to fuel jet velocities of V_j = 1 m/s, V_j = 2.5 m/s, and V_j = 5 m/s

3.3.1. Temperature distribution graph along the spray jet

- Case Re_a = 1000

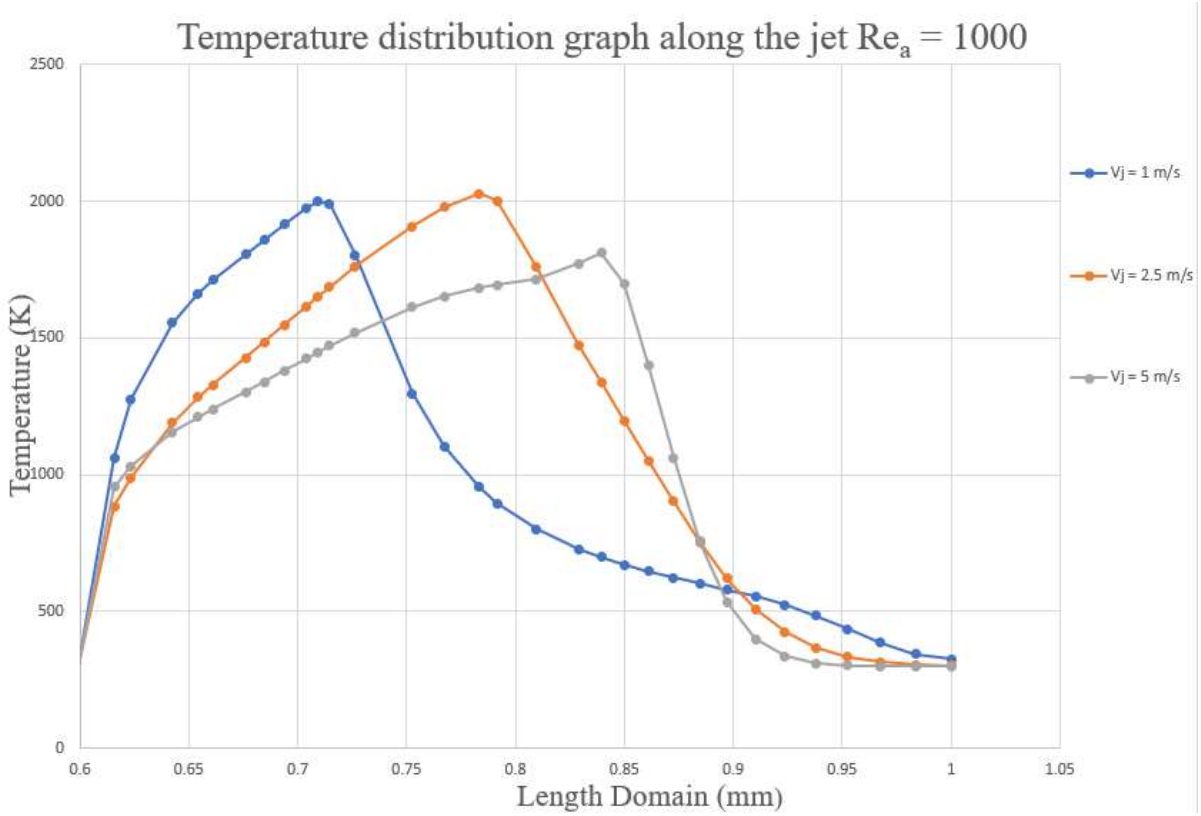

Figure 3.25 Temperature distribution graph along the jet Re_a = 1000

For the case with Reynolds number Re_a = 1000, corresponding to an air velocity Va = 1.5 m/s, based on the obtained graphs, it can be observed that the temperature distribution trend depends on the fuel jet velocity. As the fuel jet velocity increases, the temperature distribution region or the combustion zone tends to shift farther downstream, with the farthest distance observed at Vj = 5 m/s and the closest at Vj = 1 m/s. This behavior has been confirmed through the simulation results.

A higher fuel jet velocity improves flame stability, although the peak temperature may slightly decrease when the fuel velocity is high. As shown in the graph, when the fuel jet velocity reaches Vj = 5 m/s the highest among the three cases, the maximum temperature is actually lower compared to the other two cases. This is because the increased fuel velocity leads to a significant rise in momentum, which enhances the mixing process. As a result, the combustion zone becomes more widespread, and the heat is more evenly distributed rather than concentrated in one spot. Consequently, the peak temperature in the high-velocity case is lower than in the others.

- Case Re_a = 5000

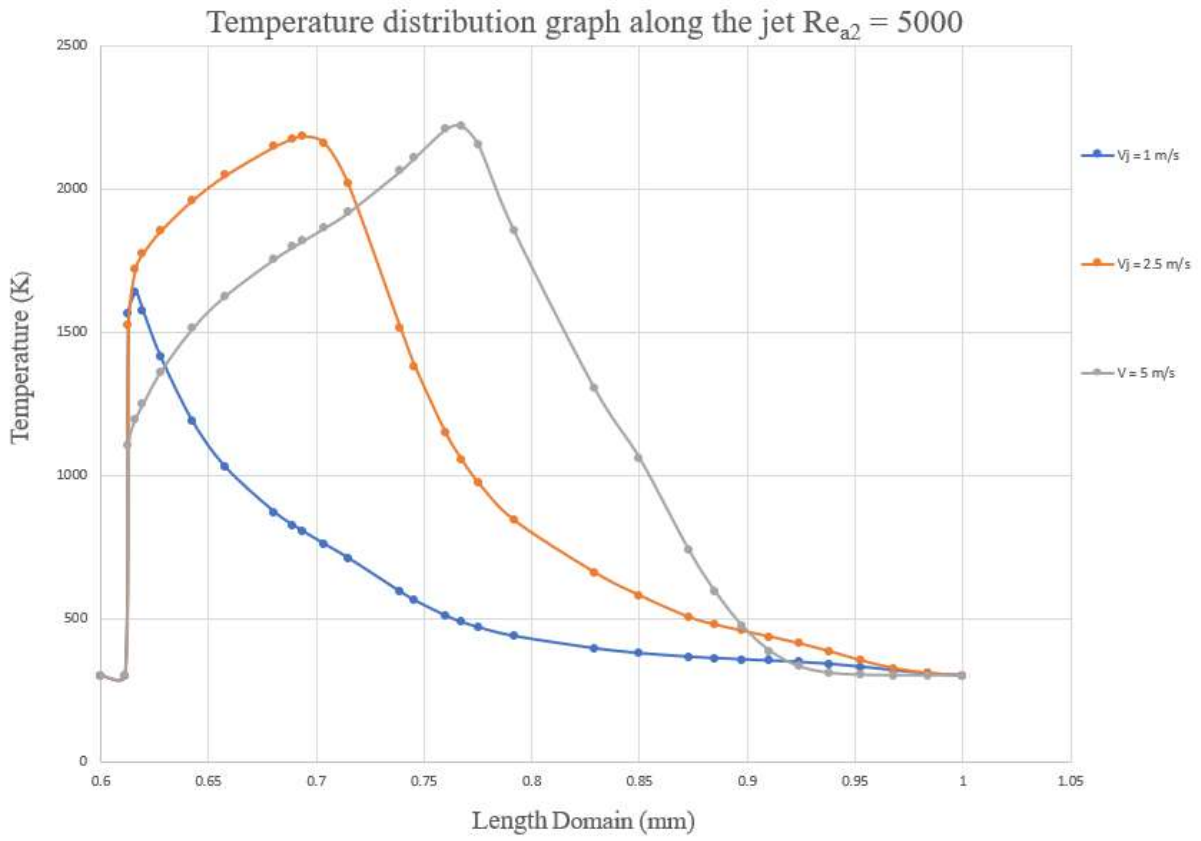

Figure 3.26 Temperature distribution graph along the jet Re_a = 5000

In the case of a Reynolds number Rea = 5000, which corresponds to an air velocity of Va = 7.5 m/s significantly higher than the fuel jet velocities in all three scenarios the temperature distribution also increases. As illustrated in the graph, when the air velocity is high, the temperature field expands, and this expansion continues with increasing fuel jet velocity, following a similar trend as observed in the case of Rea = 1000.

However, when comparing the two cases of Rea = 1000 and Rea = 5000 in terms of temperature distribution along the vertical axis of the jet, it can be observed that in the Rea = 1000 case. where the velocity ratio between the air and fuel streams ranges from 1.5 to 0.3 the high-temperature region is maintained over a longer distance along the jet axis. This indicates a more efficient heat transfer process. Since the air stream is weaker, the mixing process between fuel and air occurs more slowly. As a result, the fuel tends to burn more extensively toward the downstream region, leading to an elongated high-temperature zone. Although the peak temperature is lower, the extent of heat spread is significantly greater.

In the case of Rea = 5000, where the velocity ratio between the air and fuel streams ranges from 7.5 to 1.5, the temperature distribution region is smaller compared to Rea = 1000. However, the peak temperatures in the two fuel velocity cases of Vj = 2.5 m/s and Vj = 5 m/s are higher. This can be explained by the significantly higher air velocity in the Rea = 5000 case, which leads to faster mixing between air and fuel. The higher diffusion rate causes the combustion process to occur earlier and more concentrated near the nozzle, resulting in higher local peak temperatures. Additionally, the higher air velocity may also carry the combustion products away more quickly, diluting the overall temperature and shortening the temperature distribution region. As a result, the high-temperature zone does not extend as far downstream as in the Rea = 1000 case.

3.3.2. CO_2 concentration distribution graph along the spray jet

Based on the simulation data, the CO_2 concentration distribution along the injector axis was plotted for both Rea = 1000 and Rea = 5000 cases.

- Case Re_a = 1000

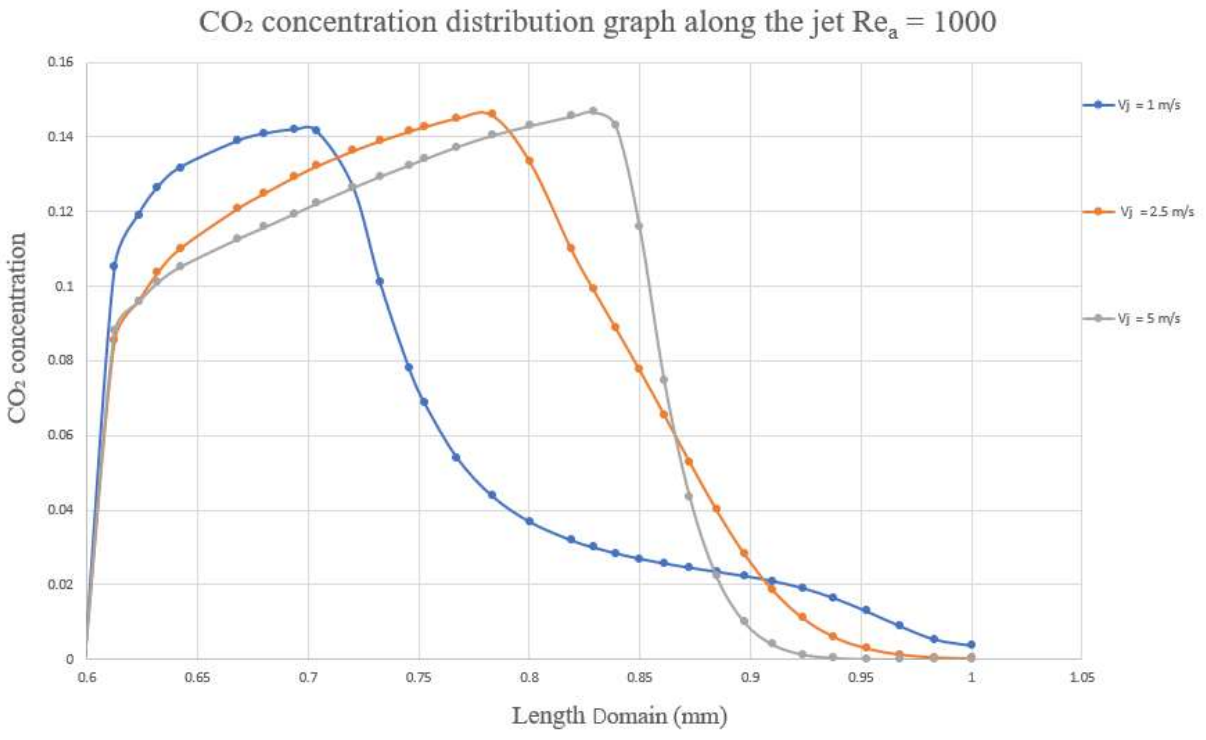

Figure 3.27 CO_2 concentration distribution graph along the jet Re_a = 1000

In general, the CO_2 concentration distribution graph closely resembles the temperature distribution graph; however, the CO_2 concentration specifically reflects pollutant emission levels. In the case of Rea = 1000, the CO_2 concentration tends to

increase initially, reaching a peak in the middle of the domain (approximately from 0.70 to 0.85 mm), and then sharply decreases toward near zero at the end of the domain.

At the fuel velocity of Vj = 1 m/s, the CO_2 concentration reaches its peak early and then rapidly decreases, indicating that the mixing and combustion processes occur quickly but lack stability and do not sustain over a long distance.

In the two cases with fuel velocities of Vj = 2.5 m/s and Vj = 5 m/s (represented by the orange and gray lines), the peak CO_2 concentration shifts further downstream. At the same time, the peak value is slightly higher, and the distribution is broader.

- Case Re_a = 5000

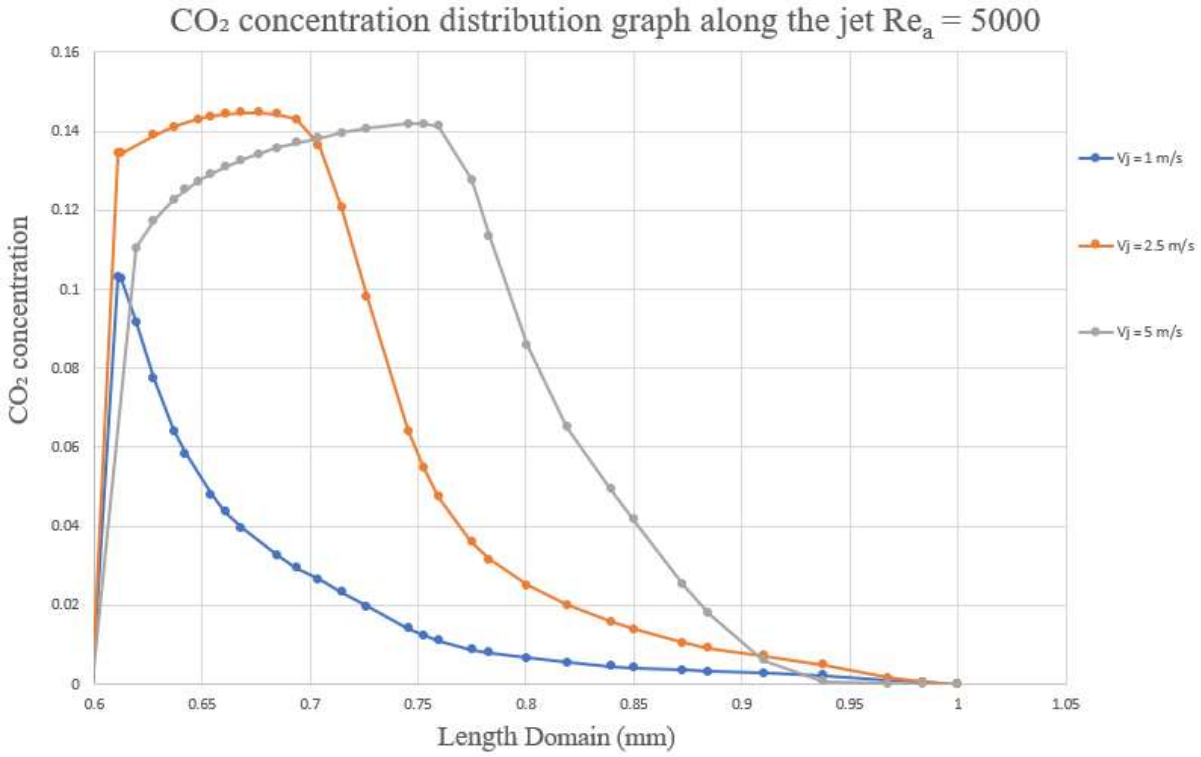

Figure 3.28 CO_2 concentration distribution graph along the jet Re_a = 5000

For the case with Reynolds number Rea = 5000, all CO_2 concentration curves reach their peak values earlier (starting from around 0.65 mm) and decrease more rapidly toward the end of the domain. Among them, only the curve for the fuel velocity Vj = 1 m/s shows a lower CO_2 concentration compared to the other two cases.

From the two CO_2 concentration distribution graphs at Rea = 1000 and Rea = 5000, it can be observed that the regions with high CO_2 concentration at Rea = 1000 indicate a higher level of pollutant emissions and show strong correlation with the temperature field distribution. As the Reynolds number increases, the stronger airflow

causes the flame region to become shorter, but the combustion intensity increases, as reflected by the higher peak temperatures. However, in terms of CO_2 concentration, in the case of Rea = 5000. where the velocity ratio of air to fuel ranges from 3 to 1.5 the combustion efficiency does not necessarily improve, and the CO_2 emission level is nearly the same as that in the Rea = 1000 case.

Moreover, the velocity of the air stream also significantly enhances the mixing process. As the airflow velocity increases, the associated kinetic energy becomes greater, which accelerates both the mixing and combustion processes. Therefore, when the velocity ratio of the air stream to the fuel stream increases, the combustion region and the CO_2 emission concentration tend to shift closer to the secondary bluff body. This trend is clearly observed in the simulation cases as well as in the temperature and CO_2 concentration distribution graphs.

3.3.3. Velocity distribution graph along the spray jet

- Case Re_a = 1000

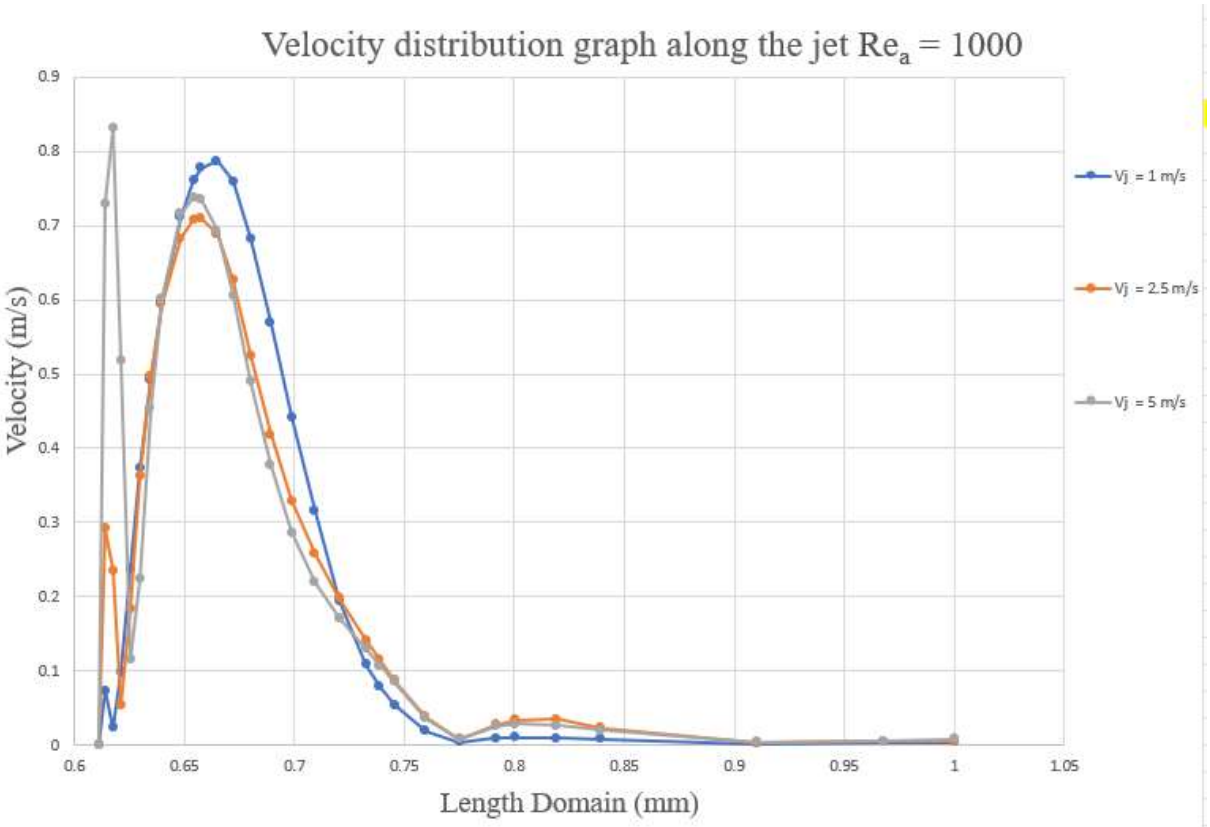

Figure 3.29 Velocity distribution graph along the jet Re_a = 1000

According to the velocity distribution graph along the jet axis in the case of Rea = 1000, where the airflow velocity V_a = 1.5 m/s, when the fuel is injected and interacts with the surface of the secondary bluff body, the velocity near the center of the disk

becomes zero. Therefore, at position 0.61, all three velocity profiles are zero on the graph. Immediately afterward, the velocities increase again as the flow passes the bluff body. In this simulation case, a pressure difference exists on the upper surface of the secondary bluff body, causing the air to flow backward and act on the top of the disk. This reverse flow, combined with the fuel velocity, generates vortices that enhance the mixing between air and fuel. In cases with higher fuel velocity, the vortex is more strongly supported. After the velocity drops to zero due to the interaction with the bluff body, it then increases rapidly in order of increasing fuel velocity.

Because the vortex absorbs a portion of the airflow's momentum, it is reflected in the domain between 0.65 and 0.7, where the velocity distribution for the fuel velocity case V_j = 1 m/s reaches the highest value.

- Case Re_a = 5000

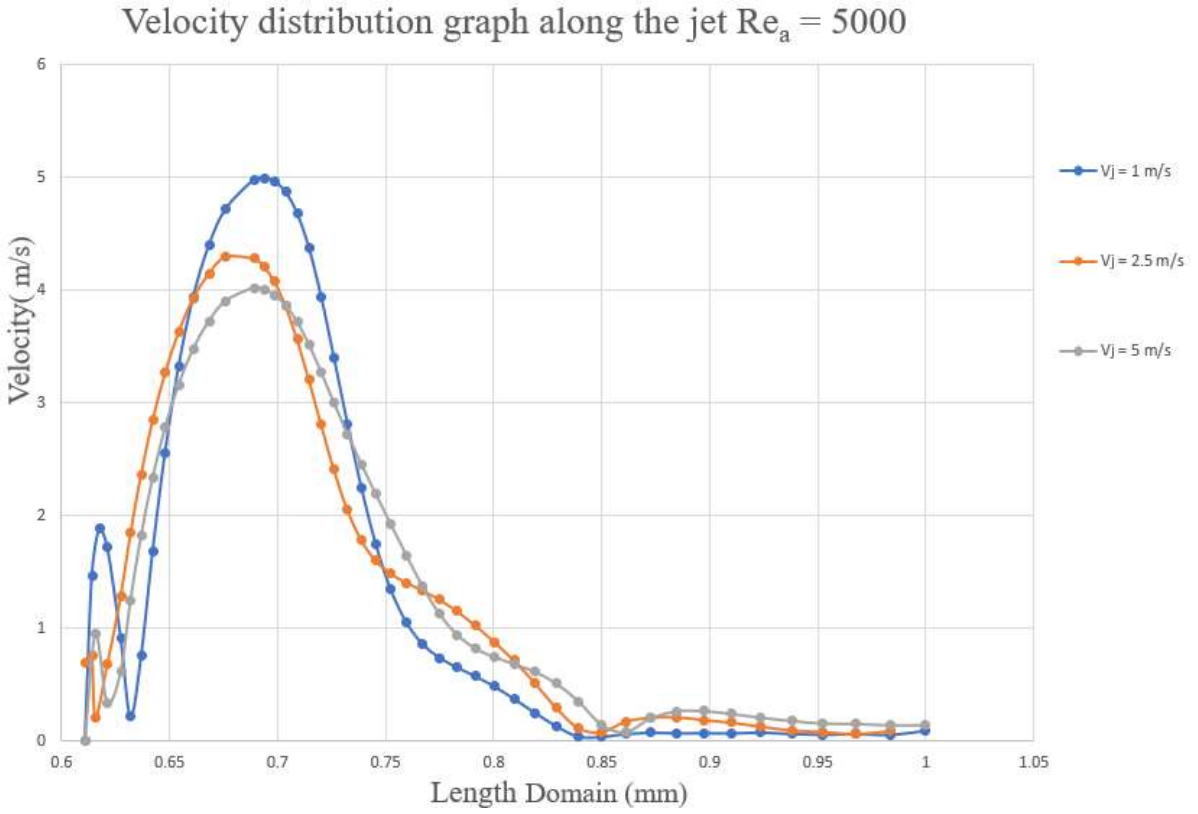

Figure 3.30 Velocity distribution graph along the jetRe_a = 5000

According to the velocity distribution graph along the spray axis in the case of Rea = 5000, where the air velocity is Va = 7.5 m/s, all three velocity curves are zero at position 0.61 in the domain, similar to the first case. However, after passing the secondary bluff body, the upper surface of the bluff body is subjected to high-speed airflow, creating a large pressure difference between the front and back of the disk. This

causes the airflow to be directed toward the disk surface and then outward toward the rim of the secondary bluff body. At this point, the upward-injected fuel is reflected back, generating an intense forced vortex in this region. The fuel stream is more strongly "entrained" by the high-speed air vortex. However, when the fuel jet velocity is high, its larger inertia resists the suction effect of the vortex. As a result, in the domain range from 0.65 to 0.75, the velocity distribution along the spray axis shows that cases with higher fuel velocity exhibit lower velocity values in this region, and vice versa.

3.4. Comparison of Velocity Field and Streamlines Between Continuous Injection and Pulsed Injection Modes

The continuous jet injection model was developed to analyze the kinematic characteristics and the mixing process between fuel and air under airflow conditions. To evaluate the efficiency and characteristics of the continuous injection mode, the simulation results are compared with a previous study that applied a pulsed injection mode using the same dual-nozzle configuration [13]. The comparison between the continuous and pulsed injection simulation results is presented in the following table:

Table 3.1 Comparison cases of continuous and pulsed simulation results

<table>
<tr><th>Comparison Case</th><th colspan="2">Injection Mode</th><th>Air Reynolds Number Re_a</th><th>Fuel Velocity V_j (m/s)</th><th>Comparison Criteria</th></tr>
<tr><td rowspan="4">Case 1</td><td colspan="2">Continuous</td><td rowspan="4">1000</td><td rowspan="4">0.5</td><td rowspan="4">Velocity contours and Velocity Streamlines</td></tr>
<tr><td rowspan="3">Pulsed</td><td>f = 20 Hz</td></tr>
<tr><td>f = 50 Hz</td></tr>
<tr><td>f = 100 Hz</td></tr>
<tr><td rowspan="4">Case 2</td><td colspan="2">Continuous</td><td rowspan="4">1000</td><td rowspan="4">1</td><td rowspan="4">Velocity contours and Velocity Streamlines</td></tr>
<tr><td rowspan="3">Pulsed</td><td>f = 20 Hz</td></tr>
<tr><td>f = 50 Hz</td></tr>
<tr><td>f = 100 Hz</td></tr>
</table>

3.4.1. Comparison of case 1

Parameter	Velocity contours	Velocity Streamlines
Continuous (time step = 100)	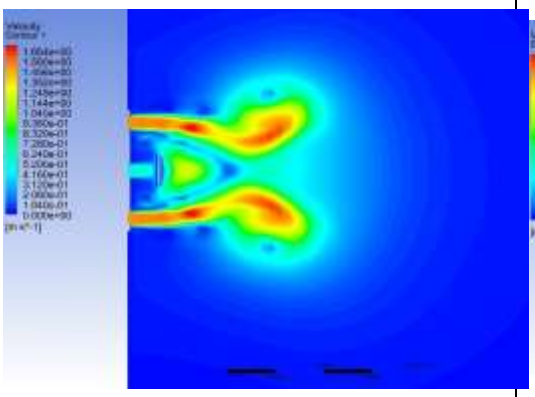	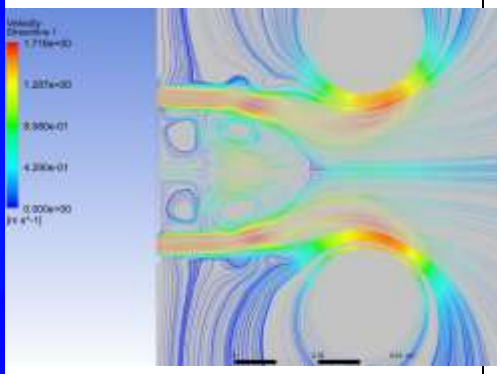
Pulsed injection at a frequency of f = 20 Hz (time step = 100)	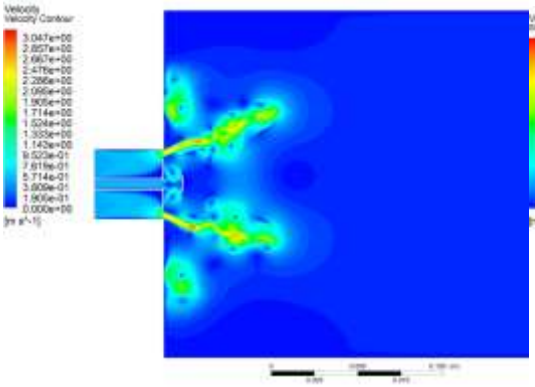	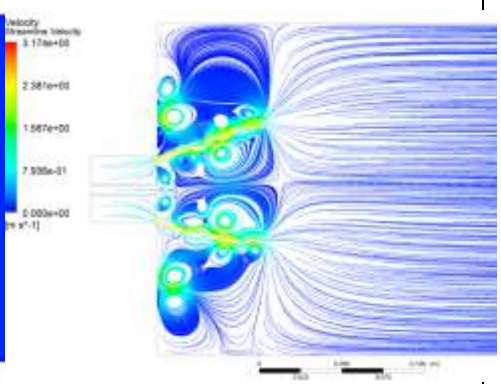
Pulsed injection at a frequency of f = 50 Hz (time step = 100)	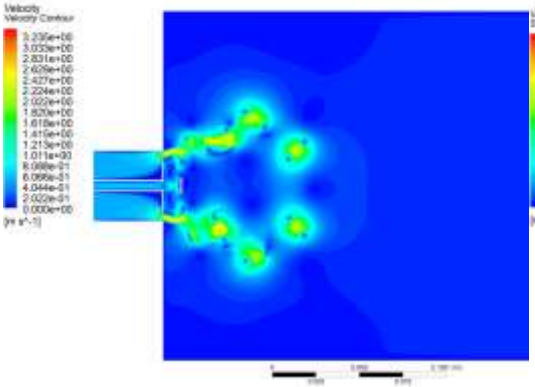	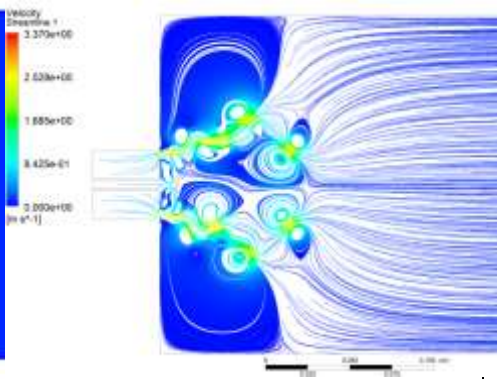
Pulsed injection at a frequency of f =100 Hz (time step = 100)	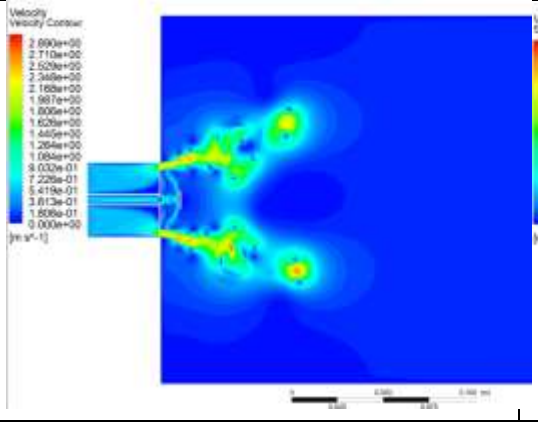	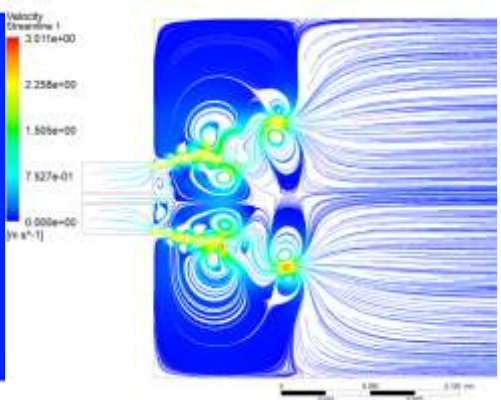

From the results of the simulation cases, it is shown that in the continuous jet mode, the flow structure is stable and clearly symmetric. The velocity distribution is smooth and uniform throughout the domain, particularly in the case of Rea = 1000 and fuel velocity V_j = 0.5 m/s.

With the velocity parameter V_j = 0.5 m/s, the simulation results show that only four vortices are formed in the velocity streamlines: two vortices near the secondary bluff body and two more below it. Due to the limited vortex formation, the mixing process mainly occurs below and around the bluff body. As the air and fuel flow upward, the lack of vortex support leads to incomplete combustion, thereby reducing thermal efficiency.

In the case of pulsed injection with the initial frequency of f = 20 Hz, the flow structure begins to form vortices, although with limited symmetry. As the pulse frequency increases from 50 Hz to 100 Hz, the vortices become larger and more widespread, gradually developing into a dense, complex, and expansive vortex structure at f = 100 Hz. It can be observed that at f = 20 Hz, vortices start to appear and spread to both sides of the jet, increasing the level of local turbulence. At f = 50 Hz, the vortex structures become more pronounced, with a significant increase in both size and number of vortices, resulting in improved mixing and momentum exchange with the surrounding environment. Particularly at f = 100 Hz, the jet becomes highly turbulent, with numerous small, interwoven vortices. The streamlines are strongly separated and distorted, indicating intense spreading and superior mixing capability compared to the other injection modes.

To ensure accuracy in the comparison between the two injection modes, an additional comparison case is conducted.

3.4.2. Comparison of case 2

Parameter	Velocity contours	Velocity Streamlines
Continuous (time step = 100)	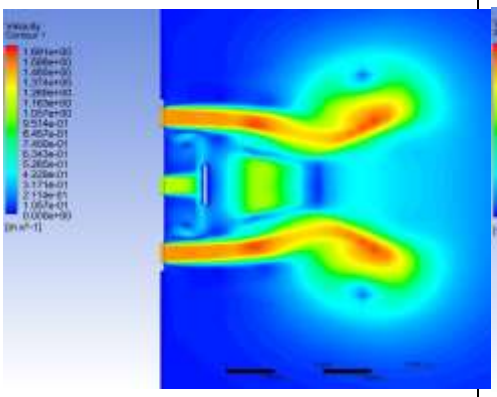	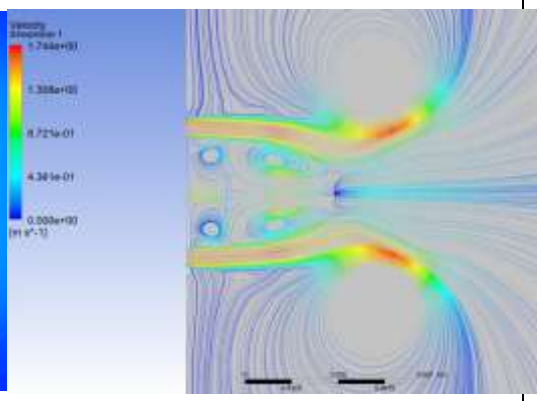
Pulsed injection at a frequency of f = 20 Hz (time step = 100)	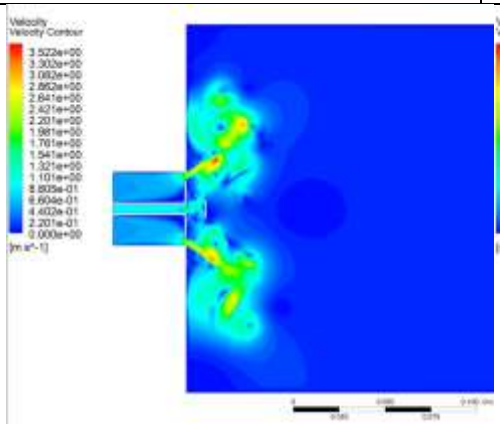	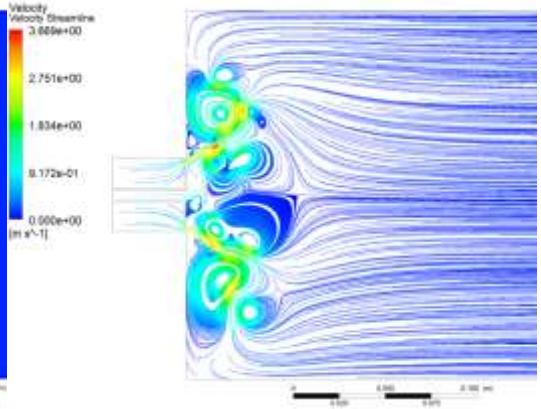
Pulsed injection at a frequency of f = 50 Hz (time step = 100)	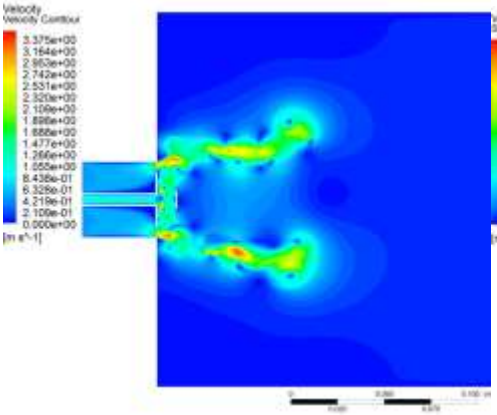	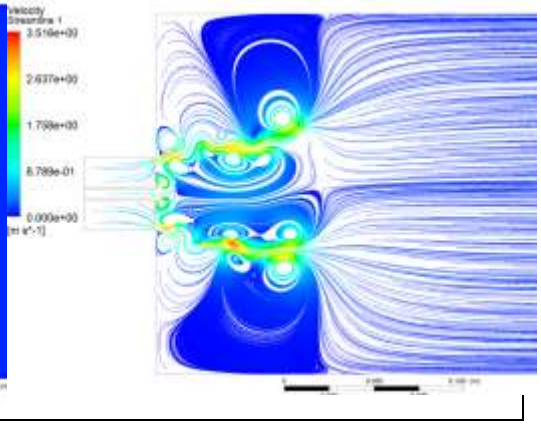

Pulsed injection at a frequency of f = 100 Hz (time step = 100)	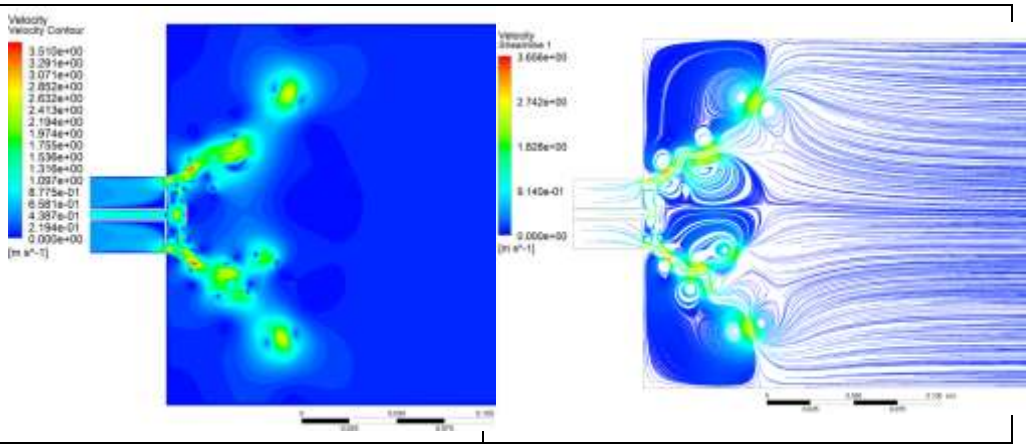

In the case of fuel jet velocity V_j = 1 m/s and Re_a = 1000, a clear distinction is observed between the continuous injection mode and the pulsed injection modes at different frequencies. Under continuous injection, the flow exhibits high stability, with a uniformly distributed velocity field. The jet develops linearly with a narrow region of influence and gradually diminishes downstream of the secondary disk.

In the pulsed injection mode, the jet becomes more unstable and distinct vortex structures form around the disk impingement region. At a frequency of f = 20 Hz, the turbulence is mild, and vortex clusters begin to form but remain indistinct. As the frequency increases to f = 50 Hz, turbulence intensifies, and symmetrical vortex structures develop, enhancing the mixing between the fuel jet and the surrounding air. Notably, at f = 100 Hz, the vortex density becomes significantly higher and more complex, with the flow exhibiting strong turbulence. The velocity field shows pronounced dispersion, indicating a higher gas diffusion capability compared to lower frequencies.

The pulsed injection mode, as the frequency increases, demonstrates superior fuel mixing and dispersion efficiency. However, it also results in a more unstable flow, enhancing the turbulence intensity and mixing effectiveness of the jet. At the same time, it significantly alters the flow's dynamic characteristics, which serves as an important basis for optimizing the combustion process.

CHAPTER 4: CONCLUSION AND FUTURE STUDY

4.1. Conclusion

After simulating the mixing and combustion processes in the dual-jet nozzle model at various air-to-fuel velocity ratios using ANSYS Fluent 19.2, several conclusions can be drawn from the results as follows:

- Velocity ratio between the fuel and air streams strongly affects the penetration depth of the fuel jet:

- When the velocity ratio between the fuel and air streams increases, meaning the fuel stream has a higher velocity, the momentum of the jet increases, allowing the spray to penetrate deeper and expand its influence toward the middle and rear regions behind the bluff body. However, an excessively high ratio can destabilize the vortex structure and reduce the effectiveness of mixing
- A velocity ratio of air to fuel in the range of 0.4 to 0.5 is suitable to ensure sufficient jet penetration while maintaining a stable vortex region to promote effective mixing.
- As the velocity ratio of air to fuel decreases, although the peak temperature drops in each case, the overall temperature distribution area increases significantly, as shown through simulation cases and corresponding graphs. Along with this, when the air-to-fuel velocity ratio decreases, the CO_2 concentration distribution also increases similarly to temperature, resulting in higher pollutant emissions.

- The influence of injection mode on flow structure and mixing capability:

- The continuous injection mode creates a relatively stable velocity field, with a narrow affected region and low propagation speed. However, its ability to generate vortices and mix fuel with air is limited, as the number of vortical regions assisting in fuel-air mixing is low, resulting in reduced mixing efficiency.
- In comparison, the pulsed injection mode (with frequencies f = 20, 50, 100 Hz) generates distinct vortex clusters from the region near the nozzle exit to the area behind the bluff body, enhancing turbulence and fuel dispersion. It can be understood that the higher the pulsing frequency, the greater the mixing effectiveness—particularly at f = 100 Hz, where strong and more evenly distributed vortices appear throughout the flow domain.

Additionally, it is evident that the bluff body in the dual-jet nozzle model plays a crucial role in influencing the flow structure, vortex generation, and mixing efficiency. Thereby directly affecting the combustion process and the overall performance of the system.

4.2. Future Study

Although the study has initially simulated and evaluated the influence of the velocity ratio between fuel and air streams as well as injection modes on the mixing and combustion processes in the dual-jet nozzle model, there are still many directions for further research as follows:

- Optimize the geometry of the nozzle and the bluff body; analyze the influence of the bluff body shape (flat, concave, convex), the distance between nozzle stages, and the nozzle hole diameter on vortex formation and the maintenance of a stable combustion zone.
- Conduct experiments to compare with simulation results; build a scaled-down experimental model to validate the CFD simulation results, thereby increasing the reliability of the research model.
- Study the influence of inlet pressure and temperature; analyze different boundary conditions to better simulate real conditions in high-pressure combustion environments (such as in gas turbines, jet engines, etc.).

REFERENCES

[1] Nguyễn Tất Tiến (2003), Nguyên Lý Động Cơ Đốt Trong, Nhà xuất bản Giáo dục.

[2] Vũ Duy Quang (2006),Thủy Khí Động Lực Học Ứng Dụng, Nhà xuất bản xây dựng Hà Nội.

[3] Nguyễn Thống(2019), Giáo trình Cơ Học Chất Lỏng, Nhà xuất bản xây dựng.

[4] Combustion Theory"(1985) – Forman A. Williams

[5] "*Computational Fluid Dynamics: The Basics with Applications* "(1995)– John D. Anderson

[6] "Computational Methods for Fluid Dynamics" (2002)– Joel H. Ferziger & Milovan Perić:

[7] ANSYS Fluent 19.2 Theory Guide (2019).

[8] Minh Duc Le, Ching Min Hsu, and Rong Fung Huang, " Flow Characteristics and Velocity Fields of Swirling Double-concentric Jets at High Central Jet Reynolds Numbers" 2018

[9] Rong Fung Huanga, Le Minh Duc, Ching Min Hsu, "Flow and Mixing Characteristics of Swirling Doubleconcentric Jets Modulated by a Dual-disk Controller" 2015

[10] Le Minh Duc, Ching Min Hsu và Rong Fung Huang, "Velocity fields and mixing properties of swirling double-concentric jets using two separated circular disks as center bodies" 2017

[11] Rong Fung Huang, Le Minh Duc và Ching Min Hsu, " Effects of swirling strength on flow characteristics of swirling double-concentric jets with a dual-disk flow controller" 2015

[12] Le Minh Duc, Ching Min Hsu và Rong Fung Huang, 'Swirling dual-disk double-concentric jets at low annulus Reynolds numbers" 2017

[13] Phan Minh Quang, "NGHIÊN CỨU ĐỘNG HỌC TIA XUNG NHỊP KẾT HỢP ĐĨA CẢN KÉP BẰNG PHƯƠNG PHÁP MÔ PHỎNG SỐ LES (LARGE EDDY SIMULATION)," Đồ án tốt nghiệp Khóa 2017, ngành KTCK – chuyên ngành CKĐL, 2022.